

Photon distribution amplitudes and light-cone wave functions in chiral quark models

Alexander E. Dorokhov*

Joint Institute for Nuclear Research, Bogoliubov Laboratory of Theoretical Physics, 114980, Moscow region, Dubna, Russia

Wojciech Broniowski[†]

*Institute of Physics, Świętokrzyska Academy, PL-25406 Kielce, Poland and
H. Niewodniczański Institute of Nuclear Physics, PL-31342 Kraków, Poland*

Enrique Ruiz Arriola[‡]

*Departamento de Física Atómica, Molecular y Nuclear,
Universidad de Granada, E-18071 Granada, Spain*

(Dated: July 14, 2006)

The leading- and higher-twist distribution amplitudes and light-cone wave functions of real and virtual photons are analyzed in chiral quark models. The calculations are performed in the nonlocal quark model based on the instanton picture of QCD vacuum, as well as in the spectral quark model and the Nambu–Jona-Lasinio model with the Pauli-Villars regulator, which both treat interaction of quarks with external fields locally. We find that in all considered models the leading-twist distribution amplitudes of the real photon defined at the quark-model momentum scale are constant or remarkably close to the constant in the x variable, thus are far from the asymptotic limit form. The QCD evolution to higher momentum scales is necessary and we carry it out at the leading order of the perturbative theory for the leading-twist amplitudes. We provide estimates for the magnetic susceptibility of the quark condensate χ_m and the coupling $f_{3\gamma}$, which in the nonlocal model turn out to be close to the estimates from QCD sum rules. We find the higher-twist distribution amplitudes at the quark model scale and compare them to the Wandzura-Wilczek estimates. In addition, in the spectral model we evaluate the distribution amplitudes and light-cone wave functions of the ρ -meson.

PACS numbers: 12.38.Lg, 11.30, 12.38.-t

Keywords: photon and ρ -meson distribution amplitudes and light-cone wave functions, magnetic susceptibility of the quark condensate, QCD, chiral quark models, instantons

I. INTRODUCTION

Investigations of hard exclusive processes are essential for our understanding of the internal quark-gluon dynamics of hadrons. Theoretically, such studies are based on the assumption of factorization of dynamics at long and short distances. The short-distance physics is well elaborated by perturbative methods of QCD and depends on particular hard subprocesses. The long-distance dynamics is essentially nonperturbative and within the factorization formalism becomes parametrized in terms of hadronic *distribution amplitudes* (DAs) or their transverse-momentum unintegrated generalizations, the *light-cone wave functions* (LCWF)¹. These nonperturbative quantities are universal and are defined as vacuum-to-hadron matrix elements of particular nonlocal light-cone quark or quark-gluon operators. The evolution of DAs at sufficiently large virtuality q^2 is controlled by the renormalization scale dependence of the quark bilinear operators within the QCD perturbation theory. For leading-order DAs this dependence is governed by simple QCD evolution equations of the Efremov-Radyushkin-Brodsky-Lepage (ER-BL) type [2, 3, 4, 5, 6]. When the normalization scale goes to infinity the DAs reach an ultraviolet fixed point and are uniquely determined by perturbative QCD. However, the derivation of the DAs themselves at an initial scale μ_0^2 from first principles is a nonperturbative problem and remains a serious challenge. Moreover, at experimentally achievable energies it is likely that the normalization scale is low and the nonperturbative effects are essential. It is expected that at such low scales the shape of DAs can differ essentially from their asymptotic forms and at present can not be strictly predicted from first principles. Nevertheless, there are several well-established methods to get information on genuinely

*Electronic address: dorokhov@theor.jinr.ru

[†]Electronic address: Wojciech.Broniowski@ifj.edu.pl

[‡]Electronic address: earriola@ugr.es

¹ For a recent review see, *e.g.*, [1].

nonperturbative quantities such as hadronic distribution amplitudes at low normalization scale: the QCD sum rules method [7, 8, 9, 10, 11], the relativistic quark models [12], the instanton liquid model [13, 14, 15, 16, 17], the effective chiral quark models [18, 19], or transverse lattice QCD [20]. First and second moments of pion DAs have also been evaluated on Euclidean lattices [21, 22, 23].

A special class of processes involves either virtual or real photons which provide ideal tools for probing the hadronic structure in deep-inelastic and hard exclusive scattering experiments. The reason is that the photon is not an eigenstate of QCD but a superposition of the U_1 gauge boson and quark-gluon configurations which are suppressed by the electromagnetic coupling. While a photon is normally considered a structureless particle, it can fluctuate into a charged lepton- and quark-pair states, which can be revealed through interactions with a highly virtual photon. Thus, the photon DAs have both electromagnetic and hadronic components. The electromagnetic component can be calculated within QED, while the hadronic part must be analyzed with non-perturbative methods of strong interactions.

Despite the wealth of theoretical studies not much experimental information is available to constrain various theoretical predictions (for a recent review see [24]). The hadronic DAs and LCWFs can be measured from hard exclusive processes at some high momentum scale. For example the pion and photon DAs may be extracted from hard dijet production by incident pions [25, 26] and real photons [27, 28], correspondingly. The measurements of the photon DA and LCWF are based on the method of diffractive dissociation applied already to the study of the pion distributions. A differential measurement of the pion DA and LCWF was performed by the Fermilab E791 collaboration by studying the diffractive dissociation of high momentum pions into two jets [29]. The recent measurements at HERA provided the first evidence that diffractive dissociation of particles can be reliably used to measure the photon DAs. Hence, the electromagnetic component of the photon LCWF may be extracted from the study of the exclusive $ep \rightarrow ep\mu^+\mu^-$ photoproduction process [30] and the hadronic component from the exclusive processes of diffractive photo- or electroproduction of two pions [31]. This may be considered as a special case of the photon dissociation to dijets when each jet consists of one pion.

The aim of the present work is to study the photon DAs and LCWFs of leading and higher twists at a low-momentum renormalization scale in a variety of chiral quark models: the gauged non-local chiral quark model based on the instanton picture of QCD vacuum [32, 33, 34], the spectral quark model [35], and the Nambu–Jona-Lasinio model with the Pauli-Villars regulator. There are a number of advantages of the chiral model approach in comparison with other existing approaches. Besides the incorporation of spontaneous chiral symmetry breaking calculations can directly be carried out in the Minkowski space. Actually, the corresponding calculations are manifestly covariant, so the subtleties of the light-cone quantization do not arise. Within non-local models an effective resummation of quark-gluon condensates of growing dimension is performed.

Although our results are obviously model dependent, we have theoretical control on several properties that should be satisfied *a priori*, with the symmetry requirements being the most stringent restriction. The resulting Ward-Takahashi identities are properly incorporated and their role in quark models is very important when computing the light-cone properties. We stress that in our approach we depart from standard parameterizations and do undertake a *genuine dynamical calculation*. Analogous results for the pion have been obtained earlier in the instanton model [13, 17, 36], in the Nambu–Jona-Lasinio model [19], in the spectral quark model [35], and most recently in the large- N_c Regge model [37].

The paper is organized as follows: in Sect. II we give definitions of the photon DAs in different channels corresponding to the twist expansion up to the twist-4 level. Necessary information about the chiral quark models that we are going to use in the paper is given in Sect. III. In particular, the corresponding normalization constants are evaluated. Section IV contains the formalism of quark model calculations of the photon LCWF and DA and a proper identification of the low-energy matrix elements is assessed. In Sect. V we give the explicit expressions for the leading-twist photon and ρ -meson distributions, while the perturbative QCD evolution of the resulting leading-twist distributions to the relevant physical scales is carried out in Sect. VI. In Section VII the calculation of the higher twist components of the photon distributions is presented. Some technical details of calculations, in particular the treatment of regularization and the QCD evolution, are given in Appendices A - C.

II. DEFINITIONS AND NOTATIONS

The distribution amplitudes for the virtual photon are defined via the matrix elements of quark-antiquark bilinear operators taken between the vacuum and the one-photon state $|\gamma^\lambda(q)\rangle$ of momentum q and polarization vector $e_\mu^{(\lambda)}$ ².

² Our definitions and notation follow closely the works of Braun, Ball and coauthors [38, 39].

It is assumed that the quark and antiquark are separated by the distance $2z$ and the light-like limit $z^2 \rightarrow 0$ is taken at a fixed scalar product $q \cdot z$. We denote $q^2 > 0$ for space-like vectors and $q^2 < 0$ for the time-like vectors. The photon polarization is always perpendicular to q , thus we have $e^{(\lambda)} \cdot q = 0$, while for the case of the *real* photon one has in addition the condition $e^{(\lambda)} \cdot z = 0$ constraining the photon polarization to the two transverse directions.

Following Refs. [38, 39, 40, 41], we use the light-cone expansion of the matrix elements in order to define the invariant amplitudes up to the twist-4 accuracy (z^2 terms are neglected)

$$\begin{aligned} \langle 0 | \bar{q}(z) \sigma_{\mu\nu} [z, -z] q(-z) | \gamma^\lambda(q) \rangle &= i e_q \langle 0 | \bar{q} q | 0 \rangle f_{\perp\gamma}^t(q^2) \left\{ \left(e_\mu^{(\lambda)} q_\nu - q_\mu e_\nu^{(\lambda)} \right) \chi_m \int_0^1 dx e^{i\xi q \cdot z} \mathcal{A}_T(x, q^2) + \right. \\ &+ \left. \frac{e^{(\lambda)} \cdot z}{(z \cdot q)^2} (q_\mu z_\nu - z_\mu q_\nu) \int_0^1 dx e^{i\xi q \cdot z} \mathcal{B}_T(x, q^2) + \frac{1}{z \cdot q} \left(e_\mu^{(\lambda)} z_\nu - z_\mu e_\nu^{(\lambda)} \right) \int_0^1 dx e^{i\xi q \cdot z} \mathcal{C}_T(x, q^2) \right\}, \end{aligned} \quad (1)$$

$$\begin{aligned} \langle 0 | \bar{q}(z) \gamma_\mu [z, -z] q(-z) | \gamma^\lambda(q) \rangle &= e_q f_{3\gamma} f_{\perp\gamma}^v(q^2) \left\{ q_\mu \frac{e^{(\lambda)} \cdot z}{q \cdot z} \frac{f_{\parallel\gamma}^v(q^2)}{f_{\perp\gamma}^v(q^2)} \int_0^1 dx e^{i\xi q \cdot z} \mathcal{A}_V(x, q^2) + \right. \\ &+ \left. \left(e_\mu^{(\lambda)} - q_\mu \frac{e^{(\lambda)} \cdot z}{q \cdot z} \right) \int_0^1 dx e^{i\xi q \cdot z} \mathcal{B}_V(x, q^2) + z_\mu \frac{e^{(\lambda)} \cdot z}{(q \cdot z)^2} \int_0^1 dx e^{i\xi q \cdot z} \mathcal{C}_V(x, q^2) \right\}, \end{aligned} \quad (2)$$

$$\langle 0 | \bar{q}(z) \gamma_\mu \gamma_5 [z, -z] q(-z) | \gamma^\lambda(q) \rangle = e_q f_{3\gamma} f_\gamma^a(q^2) \epsilon_{\mu\nu\alpha\beta} e_\nu^{(\lambda)} q^\alpha z^\beta \int_0^1 dx e^{i\xi q \cdot z} \mathcal{D}(x, q^2), \quad (3)$$

where $\langle 0 | \bar{q} q | 0 \rangle$ is the quark condensate, χ_m is the *magnetic susceptibility of the quark condensate*, and $f_{3\gamma}$ is related to the first moment of the magnetic susceptibility. The symbol $[-z, z]$ in the matrix elements denotes the path-ordered gauge link (Wilson line) for the gluon fields between the points $-z$ and z . In the light-cone gauge, $A(z) \cdot z = 0$, assumed throughout our calculations, we have $[z, -z] = 1$ and the Wilson lines may be dropped. The integration variable x corresponds to the momentum fraction carried by the quark and $\xi = 2x - 1$ for the short-hand notation. The electric charge of the quark is denoted by e_q . For a real photon, due to condition $e^{(\lambda)} \cdot z = 0$, only four structures corresponding to the invariant amplitudes \mathcal{A}_T , \mathcal{C}_T , \mathcal{B}_V , and \mathcal{D} survive. In the present work we do not consider the twist-3 three-particle DAs which involve the gluon fields, integrated out in effective quark models.

The corresponding decay constants and form factors are defined as

$$\langle 0 | \bar{q}(0) \sigma_{\mu\nu} q(0) | \gamma^\lambda(q) \rangle = i e_q \langle 0 | \bar{q} q | 0 \rangle \chi_m f_{\perp\gamma}^t(q^2) \left(e_\mu^{(\lambda)} q_\nu - q_\mu e_\nu^{(\lambda)} \right), \quad (4)$$

$$\langle 0 | \bar{q}(0) \gamma_\mu q(0) | \gamma^\lambda(q) \rangle = e_q f_{3\gamma} f_{\perp\gamma}^v(q^2) e_\mu^{(\lambda)}, \quad (5)$$

$$\left. \frac{\partial}{\partial z_\beta} \langle 0 | \bar{q}(z) \gamma_\mu \gamma_5 [z, -z] q(-z) | \gamma^\lambda(q) \rangle \right|_{z \rightarrow 0} = e_q f_{3\gamma} f_\gamma^a(q^2) \epsilon_{\mu\nu\alpha\beta} e_\nu^{(\lambda)} q^\alpha. \quad (6)$$

The vector constant at zero virtuality, $f_{\perp\gamma}^v(q^2 = 0)$, is zero due to the conservation of the vector current. The nonperturbative constants χ_m and $f_{3\gamma}$ provide natural mass scales for the tensor and vector components of the photon DAs. In QCD the matrix elements of the relevant local operators are defined as

$$\langle 0 | \bar{q} \sigma_{\mu\nu} q | 0 \rangle_F = e_q \chi_m \langle 0 | \bar{q} q | 0 \rangle F_{\mu\nu}, \quad (7)$$

$$\left\langle 0 \left| \bar{q} g \tilde{G}_{\mu\nu} \gamma_\alpha \gamma_5 q \right| 0 \right\rangle_F = e_q f_{3\gamma} D_\alpha F_{\mu\nu}, \quad (8)$$

where $F_{\mu\nu}$ ($G_{\mu\nu}$) is the field-strength tensor of the external electromagnetic (gluon) field, D_α is the covariant derivative, and the index F indicates that the vacuum expectation values are taken in the QCD vacuum in the presence of the background field $F_{\mu\nu}$. QCD predicts the scale dependence of the quark condensate $\langle 0 | \bar{q} q | 0 \rangle$, its magnetic susceptibility χ_m , and $f_{3\gamma}$, which at the leading logarithmic approximation evolve as

$$\langle 0 | \bar{q} q | 0 \rangle_\mu = L^{-\gamma_{\bar{q}q}/b} \langle 0 | \bar{q} q | 0 \rangle_{\mu_0}, \quad \chi_m|_\mu = L^{-(\gamma_0 - \gamma_{\bar{q}q})/b} \chi_m|_{\mu_0}, \quad f_{3\gamma}|_\mu = L^{-\gamma_f/b} f_{3\gamma}|_{\mu_0} \quad (9)$$

where $L = \alpha_s(\mu^2) / \alpha_s(\mu_0^2)$ is the evolution ratio, $b = (11N_c - 2n_f) / 3$, $\gamma_{\bar{q}q} = -3C_F$ is the anomalous dimension of the quark condensate, $\gamma_0 = C_F$ is the anomalous dimension of the chiral-odd local operator of leading-twist,

$\gamma_f = 3C_A - C_F/3$, with $C_F = 4/3$ and $C_A = 3$ for $N_c = 3$. By convention, the constants are chosen in such a way that the invariant functions are normalized by conditions

$$\begin{aligned} \int_0^1 dx \mathcal{A}_T(x, q^2) &= 1, & \int_0^1 dx \mathcal{B}_T(x, q^2) &= \int_0^1 dx \mathcal{C}_T(x, q^2) = 0, \\ \int_0^1 dx \mathcal{A}_V(x, q^2) &= \int_0^1 dx \mathcal{B}_V(x, q^2) = 1, & \int_0^1 dx \mathcal{C}_V(x, q^2) &= 0, \\ \int_0^1 dx \mathcal{D}(x, q^2) &= 1. \end{aligned} \quad (10)$$

In order to define the photon DAs of definite twist it is convenient to introduce the light-like vector p_μ ($p^2 = 0$), such that

$$p_\mu = q_\mu - \frac{q^2}{2} n_\mu, \quad (11)$$

where the light-like vector

$$n_\mu = \frac{z_\mu}{p \cdot z} \quad (12)$$

is normalized by the condition $n \cdot p = 1$. Then the photon polarization vector $e_\mu^{(\lambda)}$ is decomposed into projections onto the two light-like vectors and the transverse plane as

$$e_\mu^{(\lambda)} = \left(e^{(\lambda)} \cdot n \right) p_\mu + \left(e^{(\lambda)} \cdot p \right) n_\mu + e_{\perp\mu}^{(\lambda)}. \quad (13)$$

Applying the useful relations

$$z \cdot q = z \cdot p, \quad e^{(\lambda)} \cdot p = -\frac{q^2}{2} \left(e^{(\lambda)} \cdot n \right), \quad (14)$$

it is possible to express the above definitions in the form

$$\begin{aligned} \langle 0 | \bar{q}(z) \sigma_{\mu\nu} q(-z) | \gamma^\lambda(q) \rangle &= i e_q \langle \bar{q} q \rangle f_{\perp\gamma}^t(q^2) \left\{ \left(e_{\perp\mu}^{(\lambda)} p_\nu - e_{\perp\nu}^{(\lambda)} p_\mu \right) \chi_m \int_0^1 dx e^{i\xi q \cdot z} \phi_{\perp\gamma}(x, q^2) + \right. \\ &+ \left. \left(p_\mu n_\nu - n_\mu p_\nu \right) \left(e^{(\lambda)} \cdot n \right) \int_0^1 dx e^{i\xi q \cdot z} \psi_\gamma^{(t)}(x, q^2) + \left(e_{\perp\mu}^{(\lambda)} n_\nu - n_\mu e_{\perp\nu}^{(\lambda)} \right) \int_0^1 dx e^{i\xi q \cdot z} h_\gamma^{(t)}(x, q^2) \right\}, \end{aligned} \quad (15)$$

$$\begin{aligned} \langle 0 | \bar{q}(z) \gamma_\mu q(-z) | \gamma^\lambda(q) \rangle &= e_q f_{3\gamma} f_{\perp\gamma}^v(q^2) \left\{ p_\mu \left(e^{(\lambda)} \cdot n \right) \frac{f_{\parallel\gamma}^v(q^2)}{f_{\perp\gamma}^v(q^2)} \int_0^1 dx e^{i\xi q \cdot z} \phi_{\parallel\gamma}(x, q^2) + \right. \\ &+ \left. e_{\perp\mu}^{(\lambda)} \int_0^1 dx e^{i\xi q \cdot z} \psi_{\perp\gamma}^{(v)}(x, q^2) + n_\mu \left(e^{(\lambda)} \cdot n \right) \int_0^1 dx e^{i\xi q \cdot z} h_\gamma^{(v)}(x, q^2) \right\}, \end{aligned} \quad (16)$$

$$\langle 0 | \bar{q}(z) \gamma_\mu \gamma_5 q(-z) | \gamma^\lambda(q) \rangle = e_q f_{3\gamma} f_\gamma^a(q^2) \epsilon_{\mu\nu\alpha\beta} e_\nu^{(\lambda)} p^\alpha z^\beta \int_0^1 dx e^{i\xi q \cdot z} \psi_\gamma^{(a)}(x, q^2). \quad (17)$$

The DAs $\phi_{\perp\gamma}$ and $\phi_{\parallel\gamma}$ are of twist-2, $\psi_\gamma^{(t,v,a)}$ are of twist-3, and $h_\gamma^{(t,v)}$ are of twist-4³. In the case of the real photon one has $e^{(\lambda)} \cdot n = 0$ and only $\phi_{\perp\gamma}$, $\psi_{\perp\gamma}^{(v)}$, $\psi_\gamma^{(a)}$ and $h_\gamma^{(t)}$ are coupled. The leading twist functions $\phi_{\perp\gamma}(x, q^2)$ and $\phi_{\parallel\gamma}(x, q^2)$ describe the photon distribution amplitudes that a virtual photon with momentum q dissociates into a quark-antiquark pair at small transverse separation.

³ This dimensional twist-counting refers to the ‘‘dynamical’’ twist of a matrix-element, as opposed to the ‘‘geometric’’ twist of a (local) operator.

Comparing (15)-(17) with the light-cone expansions (1)-(3) one finds the following relations between the invariant amplitudes and the DAs

$$\begin{aligned}
\phi_{\perp\gamma}(x, q^2) &= \mathcal{A}_T(x, q^2), & \psi_{\gamma}^{(t)}(x, q^2) &= q^2 \chi_m \mathcal{A}_T(x, q^2) + \mathcal{B}_T(x, q^2) + \mathcal{C}_T(x, q^2), \\
h_{\gamma}^{(t)}(x, q^2) &= \frac{1}{2} q^2 \chi_m \mathcal{A}_T(x, q^2) + \mathcal{C}_T(x, q^2), \\
\phi_{\parallel\gamma}(x, q^2) &= \mathcal{A}_V(x, q^2), & \psi_{\gamma}^{(v)}(x, q^2) &= \mathcal{B}_V(x, q^2), \\
h_{\gamma}^{(v)}(x, q^2) &= \frac{1}{2} q^2 \frac{f_{\parallel\gamma}^v(q^2)}{f_{\perp\gamma}^v(q^2)} \mathcal{A}_V(x, q^2) - q^2 \mathcal{B}_V(x, q^2) + \mathcal{C}_V(x, q^2), \\
\psi_{\gamma}^{(a)}(x, q^2) &= \mathcal{D}(x, q^2).
\end{aligned} \tag{18}$$

Within the quark models it is more convenient to calculate first the invariant amplitudes and then by using the above relations the DAs themselves.

III. CHIRAL QUARK MODELS

A. Instanton-motivated nonlocal chiral quark model

The analysis in chiral quark models is carried at the one-quark-loop level, *i.e.* at leading order in the number of colors, N_c . We consider the strict chiral limit assuming zero current quark masses, $m_{u,d} = 0$. Our basic expressions are derived for the case of the *non-local chiral quark model*, discussed in detail Ref. [33, 42, 43, 44, 45]. The expressions for other models analyzed in this paper can be formally obtained from the general formulas of the non-local model.

The non-local quark models are inspired by the underlying QCD-based models, such as the instanton-vacuum model [46, 47, 48, 49], the Schwinger-Dyson resummation of the rainbow diagrams [50], and some others, which all may be cast in the form of non-local quark dynamics. The models develop, via spontaneous chiral symmetry breaking, the quark mass depending on the quark virtuality. The quark propagator has the form (following the instanton liquid model we set for simplicity the quark wave-function renormalization to unity, $Z(p) = 1$)

$$S(p) = \frac{1}{\hat{p} - M(p) + i\varepsilon}, \quad M(p) = M_0 f^2(p^2) \tag{19}$$

where the dynamical quark mass $M(p)$ is expressed via the nonlocal (in coordinate space) function $f(p)$ defining the nonlocal properties of the QCD vacuum [51, 52, 53]. We have to emphasize the essential difference of this expression compared to the usually used perturbative expression, where the effects of the spontaneous violation of the chiral symmetry are not taken into account and thus $M(p) \equiv 0$.

Throughout the paper we use the notations⁴

$$D(k) = k^2 + M(k), \quad M^{(1)}(k, k') = \frac{M(k) - M(k')}{k^2 - k'^2}, \tag{20}$$

$$k_{\pm} = k \pm \frac{1}{2}q, \quad k_{\perp}^2 = (k_+ \cdot k_-) - \frac{(k_+ \cdot q)(k_- \cdot q)}{q^2}, \tag{21}$$

and for any function F one defines $F_{\pm} = F(k_{\pm})$.

The photon-quark coupling for the incoming quark of momentum k and the outgoing quark of momentum $k' = k + q$ is equal to [44, 54]

$$\Gamma^{\mu}(k, k') = \gamma_{\mu} - (k + k')_{\mu} M_{k, k'}^{(1)} + \left(\gamma_{\mu} - \frac{q_{\mu} \hat{q}}{q^2} \right) B_V(q^2), \tag{22}$$

where the contribution of the rescattering in the ρ meson channel is taken into account by the factor [54]

$$B_V(q^2) = \frac{G_V}{1 - G_V J_V^T(q^2)} 8N_c \int \frac{d^4 k}{(2\pi)^4} \frac{f_+^V f_-^V}{D_+ D_-} \left[M_+ M_- + k_+ \cdot k_- - \frac{2}{3} k_{\perp}^2 \left(1 + M^{2(1)}(k_+, k_-) \right) + \frac{4}{3} k_{\perp}^2 \frac{f_- f^{(1)}(k_-, k_+)}{D_-} \right]. \tag{23}$$

⁴ In following the integrals over the momentum are calculated by transforming the integration variables into the Euclidean space, ($k^0 \rightarrow ik_4$, $k^2 \rightarrow -k^2$).

The polarization operator in the vector channel is given by

$$J_V^T(q^2) = -2N_c \int \frac{d^4k}{(2\pi)^4} \frac{(f_+^V f_-^V)^2}{D_+ D_-} \left[M_+ M_- + k_+ \cdot k_- - \frac{2}{3} k_\perp^2 \right]. \quad (24)$$

Importantly, the vertex (22) satisfies the Ward-Takahashi identity for the vector current,

$$q_\mu \Gamma^\mu(k, k') = S^{-1}(k) - S^{-1}(k'). \quad (25)$$

The straightforward check uses the fact that $B_V(0) = 0$ identically. The inclusion of dressed vertices is crucial for the consistency of calculations in the non-local quark models.

As argued in [54] (see also [52, 55]), it is convenient to work with the mass function corresponding to the instanton field taken in the axial gauge, where P exponential factor over nonperturbative (instanton) gluon field equals unity. In this gauge at large space-like momenta $M(p)$ must decrease faster than any inverse power of p^2 , *e.g.*, as an exponential. Below we assume for simplicity a universal gaussian form of the two nonlocal functions,

$$f(p) = f_V(p) = \exp\left(-\frac{p^2}{\Lambda^2}\right), \quad (26)$$

with p denoting the Euclidean momentum. Also in this work we do not consider for the nonlocal model the time-like region close to the resonances, such as the ρ -meson. As the model parameters we take

$$M_0 = 240 \text{ MeV}, \quad \Lambda = 1110 \text{ MeV}, \quad (27)$$

from the work [56] where they were fixed by the requirement to reproduce the chiral limit of the pion weak decay constant $f_\pi^{\text{chiral}} = 86 \text{ MeV}$ [57] and the contribution of the hadronic vacuum polarization to the anomalous magnetic moment of the muon. As found in [56], the latter is very sensitive to the value of the mass parameter M_0 , preferring lower numbers. For the vector coupling we take $G_V = -8.7 \text{ GeV}^{-2}$. In Appendix B we give further details on the properties of the Gaussian shape of nonlocality in momentum and α -representations.

Let us also mention restriction on the nonlocal models coming from consistency with the operator product expansion in QCD. It was first found in [17] that in order to guarantee correct high momenta expansion of hadronic form factors and other quantities only vertices depending on quark virtualities k^2 and k'^2 may be used. The possible forms are $f(k^2)f(k'^2)$, as it is predicted by instanton model, or more general form $f(\frac{k^2+k'^2}{2})$. The vertices containing the linear combination of quark momenta, such as $f(\frac{k+k'}{2})$, lead to exponentially growing hadronic form factors at large external momenta. The same requirement restricts possible prescriptions for the usage of the flavor P -exponents gauged with respect to external currents. We follow the prescription suggested by Mandelstam and first used within the effective models in [42]. On the other hand, the prescription used in [32] leads to a linear combination of quark momenta and results in exponentially growing asymptotics of hadronic form factors, inconsistent with the operator product expansion.

Now we are ready to compute the quantities referring to the quark bilinear matrix elements of Eq. (1-3). The normalization factors are defined as (we denote $u = k^2$)⁵

$$\langle 0 | \bar{q}q | 0 \rangle^{\text{inst}} = -N_c \int \frac{du}{4\pi^2} \frac{uM(u)}{D(u)}, \quad (28)$$

$$\chi_m^{\text{inst}} = -\frac{N_c}{\langle \bar{q}q \rangle} \int \frac{du}{4\pi^2} \frac{u(M(u) - uM'(u))}{D^2(u)}, \quad (29)$$

$$f_{3\gamma}^{\text{inst}} = -N_c \int \frac{du}{4\pi^2} \frac{M^2(u)}{D(u)}. \quad (30)$$

The above equations with parameters (27) yield

$$\begin{aligned} \langle 0 | \bar{q}q | 0 \rangle^{\text{inst}} \Big|_{\mu_{\text{inst}}} &= -(0.214 \text{ GeV})^3, & \chi_m^{\text{inst}} \Big|_{\mu_{\text{inst}}} &= 4.32 \text{ GeV}^{-2}, \\ f_{3\gamma}^{\text{inst}} \Big|_{\mu_{\text{inst}}} &= -0.0073 \text{ GeV}^2. \end{aligned} \quad (31)$$

⁵ The expression for the magnetic susceptibility has been obtained in [54, 58].

In Ref. [54] the renormalization scale typical for the instanton fluctuations was estimated as $\mu_{\text{inst}} \approx 0.53$ GeV. The estimate is made by means of comparing the value of the quark condensate with that found in QCD sum rules at standard renormalization point $\mu_0 = 1$ GeV. With Λ_{QCD} for three flavors being $\Lambda_{\text{QCD}}^{(n_f=3)} = 312$ MeV [59, 60] the evolution ratio in (9) from the scale μ_{inst} to μ_0 equals $L = 2.17$. Rescaling the values obtained in the non-local quark model to the standard renormalization point μ_0 yields

$$\begin{aligned} \langle 0 | \bar{q}q | 0 \rangle^{\text{inst}} \Big|_{\mu_0} &= -(0.24 \text{ GeV})^3, & \chi_m^{\text{inst}} \Big|_{\mu_0} &= 2.73 \text{ GeV}^{-2}, \\ f_{3\gamma}^{\text{inst}} \Big|_{\mu_0} &= -0.0035 \text{ GeV}^2. \end{aligned} \quad (32)$$

These numbers are in a rather good agreement with the estimates obtained from the QCD sum rules supplemented by the vector meson dominance technique, which provide [39]

$$\begin{aligned} \langle 0 | \bar{q}q | 0 \rangle^{\text{QCDsr}} \Big|_{\mu_0} &= -(0.24 \pm 0.02) \text{ GeV}^3, & \chi_m^{\text{QCDsr}} \Big|_{\mu_0} &= (3.15 \pm 0.3) \text{ GeV}^{-2}, \\ f_{3\gamma}^{\text{QCDsr}} \Big|_{\mu_0} &= -(0.0039 \pm 0.0020) \text{ GeV}^2. \end{aligned} \quad (33)$$

Let us also mention that the vector-meson dominance model predicts [39]

$$\chi_m^{\text{vmd}} = \frac{2}{m_\rho^2} = 3.37 \text{ GeV}^{-2}, \quad f_{3\gamma}^{\text{vmd}} = -f_\rho^2 \varsigma_{3\rho} = -(0.0046 \pm 0.0020) \text{ GeV}^2, \quad (34)$$

where $m_\rho = 770$ MeV, $f_\rho = 215$ MeV, and $\varsigma_{3\rho} = 0.10 \pm 0.05$.



FIG. 1: Diagrammatic representation of the photon-to-current transition.

The calculations of the form factors (4)-(6) consist of the evaluation of the one-loop diagram of Fig. 1, where one vertex is the photon-quark coupling $e_q \Gamma(k, k') \cdot e^{(\lambda)}(q)$, and the other vertex involves the operators $\sigma_{\alpha\beta}$, γ_μ , or $\gamma_\mu \gamma_5$. The photon DAs, discussed later on, are obtained from these one-loop diagrams with the light-cone quark momentum projection fixed. The derivation of the form factors is straightforward [54] and yields

$$f_{\perp\gamma}^t(q^2) = -\frac{N_c}{\chi_m \langle 0 | \bar{q}q | 0 \rangle} \int \frac{d^4k}{4\pi^4} \frac{1}{D_+ D_-} \left\{ \left[\frac{M_+ + M_-}{2} - \frac{k \cdot q}{q^2} (M_+ - M_-) \right] (1 + B_V(q^2) f_+^V f_-^V) - \frac{2}{3} k_\perp^2 M^{(1)}(k_+, k_-) \right\}, \quad (35)$$

$$f_{\parallel\gamma}^v(q^2) = -\frac{N_c}{f_{3\gamma}} \int \frac{d^4k}{4\pi^4} \frac{1}{D_+ D_-} \left[\left(M_+ M_- + \left[k_+ \cdot k_- - \frac{4}{3} k_\perp^2 \right]_{\text{sub}} \right) (1 + B_V(q^2) f_+^V f_-^V) - \frac{4}{3} k_\perp^2 M^{(1)}(k_+, k_-) \right], \quad (36)$$

$$f_{\perp\gamma}^v(q^2) = -\frac{N_c}{f_{3\gamma}} \int \frac{d^4k}{4\pi^4} \frac{1}{D_+ D_-} \left[\left(M_+ M_- + \left[k_+ \cdot k_- - \frac{2}{3} k_\perp^2 \right]_{\text{sub}} \right) (1 + B_V(q^2) f_+^V f_-^V) - \frac{2}{3} k_\perp^2 M^{(1)}(k_+, k_-) \right], \quad (37)$$

$$f_\gamma^a(q^2) = 1 - \frac{1N_c}{3f_{3\gamma}} \int \frac{d^4k}{4\pi^4} k_\perp^2 \left[\frac{M_+^2 - M_-^2 + M_-^2 (u_- + M_+^2)}{D_+ D_-^2} + (+ \leftrightarrow -) \right] \quad (38)$$

The subscript *sub* means that one needs to subtract the perturbative contribution corresponding to the same expression with $M(k)$ set to zero. The results are presented in Fig. 2. We note that except for f_γ^a , the form factors drop with the characteristic scale of about 1 GeV.

In the case of the real photon the one-loop calculations provide the normalization constants

$$\begin{aligned} f_{\perp\gamma}^t(0) &= 1, & f_{\perp\gamma}^v(q^2) &= O(q^2), \\ f_{\parallel\gamma}^v(0) &= 1, & f_\gamma^a(0) &= 1 - \frac{N_c}{f_{3\gamma}} \int \frac{du}{8\pi^2} \frac{M^4(u)}{D^2(u)}. \end{aligned} \quad (39)$$

The vanishing of the transverse vector part at zero q^2 is just the manifestation of the Ward-Takahashi identity. The axial constant is not zero because the spontaneous breaking of chiral symmetry is taken into account.

At large Euclidean q one has

$$\begin{aligned} f_{\perp\gamma}^t(q \rightarrow \infty) &= \frac{2}{\chi_m} \frac{1}{q^2}, & f_{\perp\gamma}^v(q \rightarrow \infty) &= O(q^{-4}), \\ f_{\parallel\gamma}^v(q \rightarrow \infty) &= -\frac{N_c}{f_{3\gamma}} \int \frac{du}{4\pi^2} \frac{uM^2(u)}{D(u)} \frac{1}{q^2}, & f_{\gamma}^a(q \rightarrow \infty) &= 1. \end{aligned} \quad (40)$$

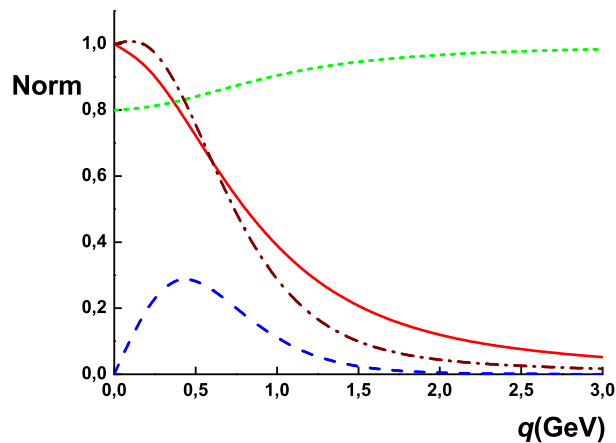


FIG. 2: Form factors associated with the photon distribution amplitude plotted as functions of the space-like momentum squared (solid line for the tensor form factor $f_{\perp\gamma}^t$, dash-dot line for the vector longitudinal form factor $f_{\parallel\gamma}^v$, dashed line for the vector transverse form factor $f_{\perp\gamma}^v$, and short-dashed line for the axial form factor f_{γ}^a).

B. Spectral quark model

The spectral quark model (SQM) is based on the spectral representation of the quark propagator [35]. The expressions for one-loop observables in SQM are obtained from the expressions of the preceding sections by replacing the quark mass with the spectral mass, $M \rightarrow \omega$, and then integrating over omega with the spectral density $\rho(\omega)$. We have

$$A = \int_C d\omega \rho(\omega) A(\omega),$$

where C is a suitably chosen contour in the complex ω plane. In the meson-dominance version of SQM [35] we have

$$\rho(\omega) = \rho_V(\omega) + \rho_S(\omega), \quad (41)$$

$$\begin{aligned} \rho_V(\omega) &= \frac{1}{2\pi i} \frac{1}{\omega} \frac{1}{(1 - 4\omega^2/M_V^2)^{5/2}}, \\ \rho_S(\omega) &= -\frac{1}{2\pi i N_c M_S^4} \frac{48\pi^2 \langle 0 | \bar{q}q | 0 \rangle}{(1 - 4\omega^2/M_S^2)^{5/2}}, \end{aligned} \quad (42)$$

where M_V is the mass of the ρ meson, and m_S provides the scale for the scalar spectral density. We note that the quark condensate is a model parameter. Matching the SQM predictions to the large- N_c results of the chiral perturbation theory in the single resonance exchange approximation allows for the identification [61]

$$M_S = M_V = m_\rho,$$

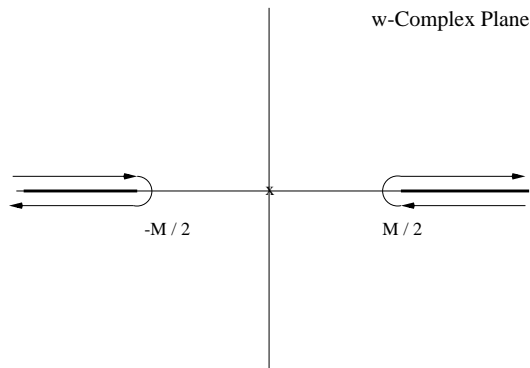


FIG. 3: The contour C for the ω -integration in the spectral quark model. M denotes the ρ -meson mass.

where m_ρ is the mass of the ρ meson. The contour C for the integration over the spectral mass ω is displayed in Fig. 3.

SQM with the meson dominance (42) generates, by construction, the monopole form of the pion electromagnetic form factor [35]. Interestingly, the model has the feature of the analytic quark confinement [62], *i.e.* the quark propagator has no poles, only cuts, in the complex momentum plane. Moreover, the evaluation of low-energy matrix elements in SQM is very simple and leads to numerous results reported in Ref. [35], in particular for the pion light-cone wave function and the pion structure functions.

The results for the normalization factors in SQM are

$$\chi_m^{\text{SQM}}|_{\mu_{\text{SQM}}} = \frac{2}{m_\rho^2} = 3.37 \text{ GeV}^{-2}, \quad f_{3\gamma}^{\text{SQM}}|_{\mu_{\text{SQM}}} = -\frac{N_c}{4\pi^2} \frac{m_\rho^2}{6} = -0.0075 \text{ GeV}^2.$$

In Ref. [35] it has been argued that the quark model scale corresponding to SQM is very low, $\mu_{\text{SQM}} = 313 \text{ MeV}$. That yields a large evolution ratio $L = 4.6$ between μ_{SQM} and $\mu_0 = 1 \text{ GeV}$, and, consequently, we find after evolution

$$\chi_m^{\text{SQM}}|_{\mu_0} = 1.37 \text{ GeV}^{-2}, \quad f_{3\gamma}^{\text{SQM}}|_{\mu_0} = -0.0018 \text{ GeV}^2,$$

much lower values than in the nonlocal model and QCD sum rule.

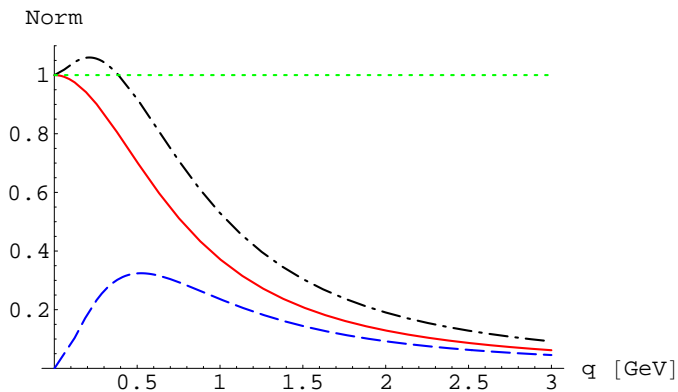


FIG. 4: Same as Fig. 2 for the spectral quark model.

For the tensor form factor we find

$$f_{\perp\gamma}^t(q^2) = \frac{m_\rho^2}{m_\rho^2 + q^2},$$

in full accordance to the vector dominance model. This makes a strong case for the assumed scalar part of the meson-dominance of spectral quark model, with the power $d_S = 5/2$ (see Ref. [35]). The tensor form factor satisfies the conditions

$$f_{\perp\gamma}^t(0) = 1, \quad f_{\perp\gamma}^t(Q^2 \rightarrow \infty) = \frac{2}{\chi_m q^2}. \quad (43)$$

For the axial form factor we find in local models $f_\gamma^a(q^2) = 1$. Expressions for the vector form factors, $f_{\gamma\parallel}^v$ and $f_{\gamma\perp}^v$ are, due to the vacuum subtraction, not analytic and the integration over the x variable has to be carried out numerically. We present these form factors for SQM in Fig. 4, noting the same qualitative behavior as for the non-local model in Fig. 2.

C. Nambu–Jona-Lasinio model

The expressions for one-loop observables in the Nambu–Jona-Lasinio model (NJL) with the Pauli-Villars regulator follow from the expressions for the non-local model. Formally, one replaces in the denominator the square of the (constant) mass, $M^2 \rightarrow M^2 + \Lambda^2$. Then, in the simplest twice subtracted case one has for any observable A the prescription

$$A = A(\Lambda^2 = 0) - A(\Lambda^2) + \Lambda^2 \frac{dA(\Lambda^2)}{d\Lambda^2}.$$

The parameters used are $M = 280$ MeV and $\Lambda = 871$ MeV, which were adjusted to yield $F_\pi = 93$ MeV. The used NJL model has no explicit coupling to vector mesons ($G_V = 0$). For the normalization factors we get

$$\begin{aligned} \langle 0 | \bar{q}q | 0 \rangle |_{\mu_{\text{NJL}}} &= \frac{N_c M}{4\pi^2} \left[\Lambda^2 - M^2 \log \left(1 + \frac{\Lambda^2}{M^2} \right) \right] = -(0.230 \text{ GeV})^3, \\ \chi_m |_{\mu_{\text{NJL}}} &= -\frac{N_c M}{4\pi^2 \langle 0 | \bar{q}q | 0 \rangle} \left[\frac{\Lambda^2}{M^2 + \Lambda^2} - \log \left(1 + \frac{\Lambda^2}{M^2} \right) \right] = 2.55 \text{ GeV}^{-2}, \\ f_{3\gamma} |_{\mu_{\text{NJL}}} &= \frac{N_c M^2}{4\pi^2} \left[\frac{\Lambda^2}{M^2 + \Lambda^2} - \log \left(1 + \frac{\Lambda^2}{M^2} \right) \right] = -0.0087 \text{ GeV}^2. \end{aligned} \quad (44)$$

The QCD evolution brings these numbers down, similarly to the case of SQM.

For the tensor form factor we find

$$f_{\perp\gamma}^t(q^2) = \frac{(M^2 + \Lambda^2) \left[2(2\Lambda^2 + S_0) \tanh^{-1} \frac{q}{\sqrt{S}} - 2\sqrt{S_0 S} \tanh^{-1} \frac{q}{S_0} + q\sqrt{S} \log \left(1 + \frac{\Lambda^2}{M^2} \right) \right]}{q\sqrt{S} \left[(M^2 + \Lambda^2) \log \left(1 + \frac{\Lambda^2}{M^2} \right) - \Lambda^2 \right]}, \quad (45)$$

$$S = 4M^2 + 4\Lambda^2 + q^2, \quad S_0 = 4M^2 + 4\Lambda^2, \quad (46)$$

which satisfies (43). Other form factors involve numerical integration. All form factors obtained in the NJL model are qualitatively very similar to the case of SQM shown in Fig. 4.

IV. PHOTON LIGHT-CONE WAVE FUNCTIONS IN QUARK MODELS

We use the light-cone coordinates with the convention $a_\pm = a_0 \pm a_3$. The null vector $n^\mu = (n^0, n^1, n^2, n^3) = (1/p_+, 0, 0, -1/p_+)$ satisfies the conditions $n^2 = 0$ and $n \cdot p = 1$, $n \cdot a = a_+/p_+$. We also denote

$$\frac{d^4 k}{(2\pi)^4} = \frac{dk_+ dk_- d^2 k_\perp}{2(2\pi)^4} \equiv d\tilde{k}.$$

The definition (15) is equivalent to (from now on we only keep the leading twist contribution)

$$ie_q \chi_m \langle \bar{q}q \rangle f_{\perp\gamma}^t(q^2) \left(q_\beta e_\alpha^{(\lambda)} - q_\alpha e_\beta^{(\lambda)} \right) \phi_{\perp\gamma}(x) = \int_{-\infty}^{\infty} \frac{d\tau}{\pi} e^{-i\tau(2x-1)} \langle 0 | \bar{q}(\tau n) \sigma_{\alpha\beta} q(-\tau n) | \gamma^\lambda(q) \rangle. \quad (47)$$

In the one loop approximation the quark model evaluation of the matrix element of the quark bilinear yields

$$\chi_m \langle \bar{q}q \rangle f_{\perp\gamma}^t(q^2) \left(q_\beta e_\alpha^{(\lambda)} - q_\alpha e_\beta^{(\lambda)} \right) \phi_{\perp\gamma}(x) = -iN_c \int d\tilde{k} \delta(k \cdot n - x) \text{Tr}[\sigma_{\alpha\beta} S(k) \Gamma \cdot e^{(\lambda)} S(k - q)], \quad (48)$$

where the trace is over the Dirac space. The interpretation of this result is clear: the photon DA times a Lorentz structure is equal to the quark-loop integral, where the $+$ -component of the momentum of one of the quarks is constrained to $k_+ = xp_+$ (see Fig. 1). If one does not carry out the transverse momentum integral in Eq. (48), then one obtains the photon *light-cone wave function*, $\Phi_{\perp\gamma}(x, k_\perp)$,

$$\chi_m \langle \bar{q}q \rangle f_{\perp\gamma}^t(q^2) \left(q_\beta e_\alpha^{(\lambda)} - q_\alpha e_\beta^{(\lambda)} \right) \Phi_{\perp\gamma}(x, k_\perp) = -iN_c \int \frac{dk_+ dk_-}{2(2\pi)^4} \delta(k \cdot n - x) \text{Tr}[\sigma_{\alpha\beta} S(k) \Gamma \cdot e^{(\lambda)} S(k - q)]. \quad (49)$$

Obviously, we have

$$\int d^2 k_\perp \Phi_{\perp\gamma}(x, k_\perp) = \phi_{\perp\gamma}(x).$$

For the twist-3 vector component of the photon light-cone wave function and DA we find from the definition (16), with analogous steps as above, the expression

$$e_{\perp\mu}^{(\lambda)} \Psi_{\gamma\parallel}^{(v)}(x, k_\perp) + q_\mu n \cdot e^{(\lambda)} \Psi_{\gamma\perp}^{(v)}(x, k_\perp) = \frac{N_c}{f_{3\gamma}} \int \frac{dk_+ dk_-}{2(2\pi)^4} \delta(n \cdot k - x) \text{Tr}[\gamma_\mu S(k) \Gamma \cdot e^{(\lambda)} S(k - q)], \quad (50)$$

while the DAs are $\psi_{\gamma i}^{(v)}(x) = \int d^2 k_\perp \Psi_{\gamma i}^{(v)}(x, k_\perp)$, with $i = (\parallel, \perp)$.

The case of the axial twist-3 component is somewhat more complicated, since the definition (17) involves a power of the coordinate z in the tensor structure. As a result we find

$$e_q f_{3\gamma} f_\gamma^a(q^2) \epsilon^{\mu\nu\alpha\beta} e_\nu^{(\lambda)} q_\alpha n_\beta \psi_\gamma^{(a)}(x) = \int_{-\infty}^{\infty} \frac{d\tau}{\pi(\tau + i\epsilon)} e^{-i\tau(2x-1)} \langle 0 | \bar{q}(\tau n) \gamma^\mu \gamma_5 q(-\tau n) | \gamma^\lambda(q) \rangle. \quad (51)$$

The one-quark loop evaluation yields

$$e_q f_{3\gamma} f_\gamma^a(q^2) \epsilon^{\mu\nu\alpha\beta} e_\nu^{(\lambda)} q_\alpha n_\beta \psi_\gamma^{(a)}(x) = \frac{4N_c}{f_{3\gamma}} \int d\tilde{k} \Theta(n \cdot k - x) \text{Tr}[\gamma^\mu \gamma_5 S(k) \Gamma \cdot e^{(\lambda)} S(k - q)]. \quad (52)$$

We may introduce the derivative of the distribution, $d/dx \psi_\gamma^{(a)}(x)$, for which we have

$$e_q f_{3\gamma} f_\gamma^a(q^2) \epsilon^{\mu\nu\alpha\beta} e_\nu^{(\lambda)} q_\alpha n_\beta \frac{d}{dx} \psi_\gamma^{(a)}(x) = \frac{4N_c}{f_{3\gamma}} \int d\tilde{k} \delta(n \cdot k - x) \text{Tr}[\gamma^\mu \gamma_5 S(k) \Gamma \cdot e^{(\lambda)} S(k - q)]. \quad (53)$$

The evaluation of this quantity is similar to the evaluation of ϕ_γ or $\psi^{(v)}$. The axial light-cone wave function is obtained from Eq. (53) if the k_\perp integration is left out, in analogy to Eqs. (49,50).

V. PHOTON LIGHT-CONE WAVE FUNCTIONS IN CHIRAL QUARK MODELS

A. Leading-twist photon DAs

The distribution amplitudes of the real photon calculated in the instanton model in the chiral limit may be cast in a closed form. It is convenient to introduce notations for the integration variables⁶

$$u_+ = u - i\lambda x, \quad u_- = u + i\lambda \bar{x}, \quad M_\pm = M(u_\pm), \quad D_\pm = D(u_\pm), \quad \bar{x} = 1 - x. \quad (54)$$

By using the definitions of Sect. IV one gets the twist-2 DA for the $\sigma_{\mu\nu}$ structure (Fig. 5)

$$\phi_{\perp\gamma}(x, q^2 = 0) = \frac{1}{\chi_m} \frac{N_c}{4\pi^2} \left[\Theta(\bar{x}x) \int_0^\infty du \frac{M(u)}{D(u)} - \int_0^\infty du \int_{-\infty}^\infty \frac{d\lambda}{2\pi} \frac{M_+ M_-}{D_+ D_-} M^{(1)}(u_+, u_-) \right]. \quad (55)$$

⁶ Some details of calculation method first developed in [15, 55] and the relevant expressions for the integrals are given in Appendix A and B.

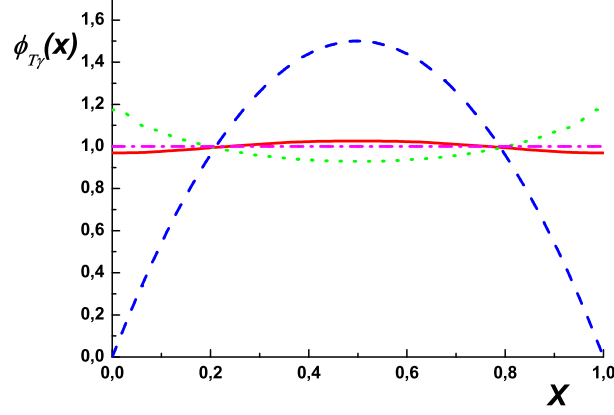


FIG. 5: The leading-twist photon distribution amplitude in the tensor channel, $\phi_{\perp\gamma}(x, q^2 = 0)$, evaluated at the quark model scale in the non-local quark model – solid line, in the spectral quark model and the NJL model (= 1) – dot dashed line, its asymptotic form – dashed line, and the result of the local approximation to the instanton model – dotted line.

Within the non-local model we can find from (55) the following light-cone wave function:

$$\Phi_{\perp\gamma}(x, \mathbf{k}_{\perp}^2, q^2 = 0) = \frac{1}{\chi_m} \frac{N_c}{4\pi^2} \left[\Theta(\bar{x}x) \frac{M(\mathbf{k}_{\perp}^2)}{D(\mathbf{k}_{\perp}^2)} - \int_{-\infty}^{\infty} \frac{d\lambda}{2\pi} \frac{M_+ M_-}{D_+ D_-} M^{(1)}(u_+, u_-) \right]. \quad (56)$$

It exhibits an exponential decay law at large \mathbf{k}_{\perp}^2 , which is a consequence of the nonlocality of the model [54] and is in accordance with the conclusion made in [63] that finiteness of all \mathbf{k}_{\perp} moments of the quark distributions guarantees the exponential fall-off of the cross sections.

In the vector channel the leading twist structure for the real photon $\phi_{\parallel\gamma}(x, q^2 = 0)$ is decoupled but the DA is not zero itself and has form

$$\phi_{\parallel\gamma}(x, q^2 = 0) = \Theta(\bar{x}x) \quad (57)$$

independently on the nonlocality shape.

The results for SQM and NJL models are obtained from (55) by taking the local limit (all derivatives are zero $M' = 0$, $M^{(1)} = 0$, etc.). This gives the result

$$\phi_{i\gamma}(x, q^2 = 0) = \Theta(\bar{x}x), \quad (58)$$

for $i = \perp, \parallel$. These leading twist DAs calculated within the instanton and local models are shown in Fig. 5 along with its asymptotic form defined at very large scale μ

$$\phi_{\perp\gamma}^{\text{asympt}}(x) = 6x\bar{x}. \quad (59)$$

In Fig. 5 there is also given the result obtained in [16] in gauge noninvariant approximation

$$\begin{aligned} \phi_{\perp\gamma}^{\text{approx}}(x) &= \frac{1}{\chi'_m} \frac{N_c}{4\pi^2} \int_0^{\infty} du \int_{-\infty}^{\infty} \frac{d\lambda}{2\pi} \frac{(1-x)M_+ + xM_-}{D_+ D_-}, \\ \chi_m^{\text{approx}} &= \frac{N_c}{4\pi^2} \int du \frac{u(M(u) - \frac{1}{2}uM'(u))}{D^2(u)} \end{aligned} \quad (60)$$

when the full vector vertex (22) is substituted by the local part. This approximation resulted in a violation of the proper normalization as implied by the Ward-Takahashi identities.

The dependence of the leading twist photon DA $\phi_{\perp\gamma}(x, q^2)$ on the photon virtuality in space-like and time-like regions is demonstrated in Fig. 6. Both leading twist DAs are normalized by unity

$$\int_0^1 \phi_{\gamma}(x, q^2) = 1. \quad (61)$$

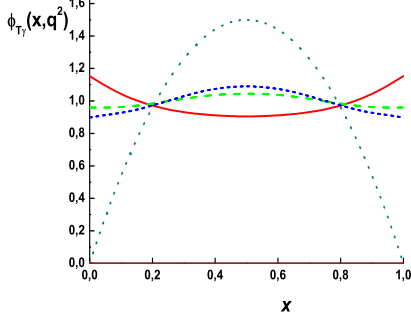


FIG. 6: Dependence of the twist-2 tensor component of the photon DA on transverse momentum squared ($q^2 = 0.25$ GeV² solid line, $q^2 = 0$ GeV² dashed line, $q^2 = -0.09$ GeV² short-dashed line, asymptotic DA - dotted line). Nonlocal model at the quark model scale.

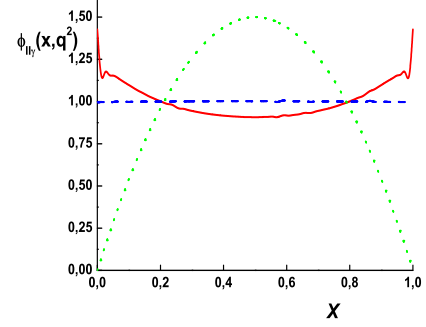


FIG. 7: Same as Fig. 6 for the twist-2 vector component of the photon DA.

At very high space-like photon virtuality the photon DA approaches the δ -function distribution concentrated at the edge points of the x interval. It corresponds to the configuration when all momenta pass through quark or anti-quark line, with other line being soft. At time-like virtualities approaching the ρ -meson pole the photon DA will be concentrated in the middle of x interval.

B. Spectral quark model

The expressions for SQM are obtained from the formulas of the preceding sections with the formal replacement $M(p) \rightarrow \omega$, and supplying the loop integrals with the addition spectral integration $\int_C \rho(\omega) d\omega$, as explained in Sect. III.B. As the result, we find the following expression for the leading-twist component of the light-cone wave function for the real photon in the tensor channel:

$$\Phi_{\perp\gamma}(x, \mathbf{k}_{\perp}) = \frac{6}{m_{\rho}^2(1 + 4\mathbf{k}_{\perp}^2/m_{\rho}^2)^{5/2}}, \quad (62)$$

Note the power-law fall-off at large transverse momenta, $\Phi_{\gamma}(x, \mathbf{k}_{\perp}) \sim 1/k_{\perp}^5$. In cross section this leads to tails of the form $\sim 1/k_{\perp}^{10}$.

For the virtual photon of virtuality q^2 , the tensor component of the light-cone wave function has the form

$$\Phi_{\perp\gamma^*}(x, \mathbf{k}_{\perp}) = \frac{6 \left(1 + \frac{q^2}{m_{\rho}^2}\right)}{m_{\rho}^2 \left(1 + 4 \frac{\mathbf{k}_{\perp}^2 + q^2 x(1-x)}{m_{\rho}^2}\right)^{5/2}}, \quad (63)$$

We also find

$$\int_0^1 dx \Phi_{\perp\gamma^*}(x, \mathbf{k}_{\perp}) = \frac{2m_{\rho}(m_{\rho}^2 + q^2)(3m_{\rho}^2 + q^2 + 12\mathbf{k}_{\perp}^2)}{(m_{\rho}^2 + 4\mathbf{k}_{\perp}^2)^{3/2}(m_{\rho}^2 + q^2 + 4\mathbf{k}_{\perp}^2)^2}. \quad (64)$$

The transverse-momentum rms is

$$\langle \mathbf{k}_{\perp}^2 \rangle \equiv \frac{\int d^2 k_{\perp} \mathbf{k}_{\perp}^2 \Phi_{\perp\gamma^*}(x, \mathbf{k}_{\perp})}{\phi_{\perp\gamma^*}(x)} = \frac{m_{\rho}^2}{2} + 2q^2 x(1-x). \quad (65)$$

For the real photon one has the estimate $\langle \mathbf{k}_{\perp}^2 \rangle = (544 \text{ MeV})^2$. For the instanton model one gets

$$\langle \mathbf{k}_{\perp}^2 \rangle \equiv \left(\int du \frac{M(u)}{D(u)} \right)^{-1} \int du \frac{uM(u)}{D(u)} = (600 \text{ MeV})^2. \quad (66)$$

For the real photon DA one finds the constant form (58), while for the virtual case we find the following normalized DA:

$$\phi_{\perp\gamma^*}(x) \equiv \int d^2k_{\perp} \Phi_{\perp\gamma}(x, \mathbf{k}_{\perp}) = \frac{\left(1 + \frac{q^2}{m_{\rho}^2}\right)}{\left(1 + 4\frac{q^2x(1-x)}{m_{\rho}^2}\right)^{3/2}}.$$

The corresponding expressions for the ρ meson are obtained by taking the limit $q^2 \rightarrow -m_{\rho}^2$, which for the DA yields

$$\phi_{\perp\rho}(x) = \delta\left(x - \frac{1}{2}\right) \quad (67)$$

This highly singular behavior is washed out by the QCD evolution, see Sect. V D.

The leading twist photon amplitude in the vector channel, $\phi_{\parallel\gamma}(x)$, is of the form given in Eq. (58), *i.e.* constant.

C. NJL model

In the NJL model one obtains the same leading-twist DAs for the real photon as Eq. (58), *i.e.* $\phi_{i\gamma}(x, q^2 = 0) = \Theta(\bar{x})$. Extension to the ρ -meson pole, however, is problematic due to appearance of the quark production threshold. For this reason we do not perform this analysis. Note that SQM is free of this problem, as no quark poles are present in this model – a feature sometimes referred to as *analytic confinement*.

D. QCD evolution

The results of the previous sections referred to the low-energy scale of the quark model, μ . In order to relate to results at higher scales, the QCD evolution is necessary. Within the effective model approach the method has been described in detail in Ref. [19] and is similar to the case of parton distribution evolution [55, 64]. For the twist-2 photon and ρ -meson DAs the leading-order QCD evolution is made on the basis of the Gegenbauer polynomials. The basic logic here is that the quark models provide the initial condition for the QCD evolution, now written as $\phi^i(x, \mu^2)$. The evolved leading-twist distribution amplitudes read [65]

$$\phi^i(x, q^2) = \phi_{\text{as}}^i(x) \sum_{n=0}^{\infty} C_n^{\lambda}(2x-1) a_n^i(q^2), \quad (68)$$

with

$$\phi_{\text{as}}^{\text{T}}(x) = \phi_{\text{as}}^{\text{V}}(x) = \phi_{\text{as}}^{\text{AV}}(x) = 6x\bar{x},$$

C_n^{λ} denoting the Gegenbauer polynomials, the prime indicating that only even n enter the sum, and $\lambda = 3/2$ for T, V, and AV. The Gegenbauer coefficients a_n^i evolve with the scale. The corresponding formulas for the leading-order QCD evolution are given in App. C. We note that the exponent in Eq. (C1) contains the difference $(\gamma_n^i - \gamma_0^i)$, such as to make the zeroth moment (the norm) of the DAs constant.

Our methods of determining the *a priori* unknown quark-model scale μ have been presented in [54] for the case of the nonlocal model and in Ref. [19] for the local models.

The numerical analysis of the evolution of the tensor DA for the photon and the ρ -meson proceeds exactly as written in the above formulas, with the series approximated by finite sums over n . Numerically, about 100 terms are needed to achieve the accuracy in the presented figures. The results for the twist-2 photon DAs are shown in Figs. 8 and 9.

The results for SQM are shown in Fig. 10. We show the evolution of the DAs for the real photon, for the ρ meson, as well as for virtual photon. We note that the evolution radically changes the character of the curves. For the real photon one starts with the flat DA of Eq. (58), exactly as for the case of the pion in the local model [19], with the evolution providing vanishing of the amplitude at the end-points and gradually approaching the asymptotic limit. So it means that all moments of the DAs evolve as continuous function, but the DA itself at some points (edge points in the discussed case) evolve discontinuously. For the ρ -meson case the result is even more dramatic, with the initial condition having the singular form of Eq. (67), evolving to broader regular functions and also tending at large evolution scales Q to the asymptotic limit. We note that this evolution is very slow. The lower part of Fig. 10 shows the DA for the virtual photon with two selected virtualities: time-like $q^2 = -m_{\rho}^2/2$ and space-like $q^2 = 2m_{\rho}^2$. We have to note that because of low initial evolution scale the QCD evolution carried out at two-loop level would give more realistic results.

The results for the real photon in the NJL model are the same as in SQM.

VI. HIGHER TWIST COMPONENTS

A. Non-leading twist photon DAs in the non-local chiral quark model

For the real photon the DAs of higher twists are following: the twist-3 transversal DA (γ_μ structure) (Fig. 11)

$$\psi_{\perp\gamma}^{(v)}(x, q^2 = 0) = \frac{1}{2} \left[\delta(x) + \delta(\bar{x}) - 2\Theta(x\bar{x}) + f_{3\gamma}^{-1} \frac{N_c}{4\pi^2} \int_0^\infty du \int_{-\infty}^\infty \frac{d\lambda (M_- - M_+)^2}{D_+ D_-} \right], \quad (69)$$

$$\int_0^1 dx \psi_{\perp\gamma}^{(v)}(x, q^2) = 0, \quad (70)$$

the twist-3 DA ($\gamma_\mu \gamma_5$ structure) (Fig. 12)

$$\psi_\gamma^{(a)}(x, q^2 = 0) = \frac{1}{f_\gamma^{(a)}(0)} \frac{N_c}{4\pi^2} \int_0^\infty du \int_{-\infty}^\infty \frac{d\lambda x M_-^2 + \bar{x} M_+^2}{D_+ D_-}, \quad (71)$$

$$\psi_\gamma^{(a)}(x=0, q^2 = 0) = \frac{f_{3\gamma}}{f_\gamma^{(a)}(0)}, \quad \int_0^1 dx \psi_\gamma^{(a)}(x, q^2) = 1, \quad (72)$$

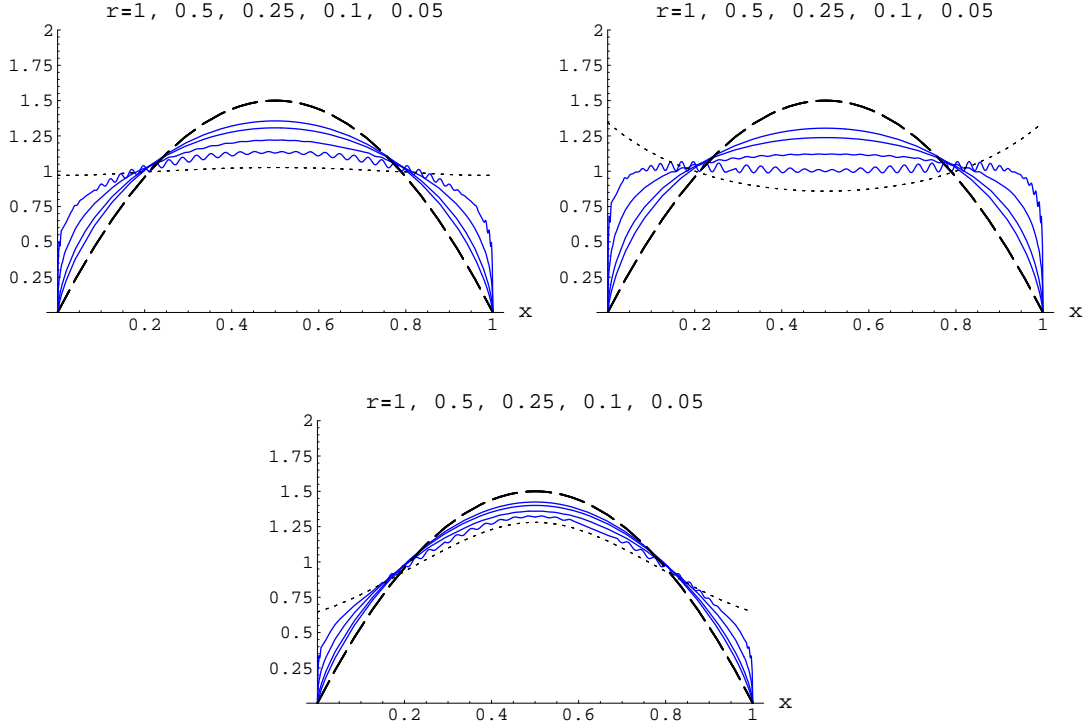


FIG. 8: The LO ERBL evolution of the nonlocal model predictions for the leading-twist *tensor* photon DA $\phi_{\perp\gamma}^{(t)}(x, q^2)$. Top left: the real photon DA, top right: the virtual photon at $q^2 = 0.25 \text{ GeV}^2$; bottom: the virtual photon at $q^2 = -0.09 \text{ GeV}^2$. The dashed lines show the asymptotic DA, $6x(1-x)$. Initial conditions, indicated by dotted lines, are evaluated in the nonlocal quark model at the initial scale $\mu^{\text{inst}} = 530 \text{ MeV}$. The solid lines correspond to evolved DA's at scales $Q = 1, 2.4, 10,$ and 1000 GeV . The corresponding values of the evolution ratio r are given in the figures. The appearance of tiny wiggles is a numerical artefact.

the twist-4 DAs ($\sigma_{\mu\nu}$ structure)

$$h_\gamma^{(t)}(x, q^2 = 0) = \frac{1}{2} \left[\delta(x) + \delta(\bar{x}) - \frac{1}{|\langle \bar{q}q \rangle|} \frac{N_c}{4\pi^2} \int_0^\infty du \int_{-\infty}^\infty \frac{d\lambda}{2\pi} \left(\frac{M_+}{D_-} + \frac{M_-}{D_+} - \frac{(M_-^2 - M_+^2)(M_- - M_+)}{D_+ D_-} \right) \right], \quad (73)$$

$$\int_0^1 dx h_\gamma^{(t)}(x, q^2) = 0,$$

$$\psi_\gamma^{(t)}(x, q^2 = 0) = h_\gamma^{(t)}(x, q^2 = 0). \quad (74)$$

In the case of Gaussian form factor (26 chosen in the present paper) the integral in (73) may be partially done as

$$\int_0^\infty du \int_{-\infty}^\infty \frac{d\lambda}{2\pi} \left(\frac{M_+}{D_-} + \frac{M_-}{D_+} \right) = \frac{M_q \Lambda^2}{2} \sum_{n=0}^\infty \frac{(-1)^n}{n!} \left(\frac{2M_q^2}{\Lambda^2} \right)^n \left[\left(\frac{\bar{x}}{x} - 2n \right)^n \Theta \left(\frac{\bar{x}}{x} - 2n \right) + (x \leftrightarrow \bar{x}) \right]. \quad (75)$$

We may compare our results with the Wandzura-Wilczek (WW) approximation which attempts to reconstruct non-leading twist result from the leading contributions. The corresponding relations for the photon deduced from the ρ -meson case [38] are

$$\psi_\gamma^{(a)WW}(x) = 2 \left[\int_0^x du \frac{\bar{x} \phi_{\parallel\gamma}(u)}{\bar{u}} + \int_x^1 du \frac{x \phi_{\parallel\gamma}(u)}{u} \right], \quad (76)$$

$$\psi_\gamma^{(v)WW}(x) = \frac{1}{2} \left[\int_0^x du \frac{\phi_{\parallel\gamma}(u)}{\bar{u}} + \int_x^1 du \frac{\phi_{\parallel\gamma}(u)}{u} \right], \quad (77)$$

$$\psi_\gamma^{(t)WW}(x) = \xi \left[\int_0^x du \frac{\phi_{\perp\gamma}(u)}{\bar{u}} - \int_x^1 du \frac{\phi_{\perp\gamma}(u)}{u} \right], \quad (78)$$

From the fact that both the nonlocal model as well as the spectral model predict for the leading twist photon DAs an almost constant function, we may predict the nonleading twist DAs as they follow from WW approximation:

$$\psi_\gamma^{(a)WW}(x) = -2(\bar{x} \ln \bar{x} + x \ln x), \quad (79)$$

$$\psi_\gamma^{(v)WW}(x) = -\frac{1}{2} \ln(x\bar{x}), \quad (80)$$

$$\psi_\gamma^{(t)WW}(x) = \xi \ln \frac{x}{1-x}. \quad (81)$$

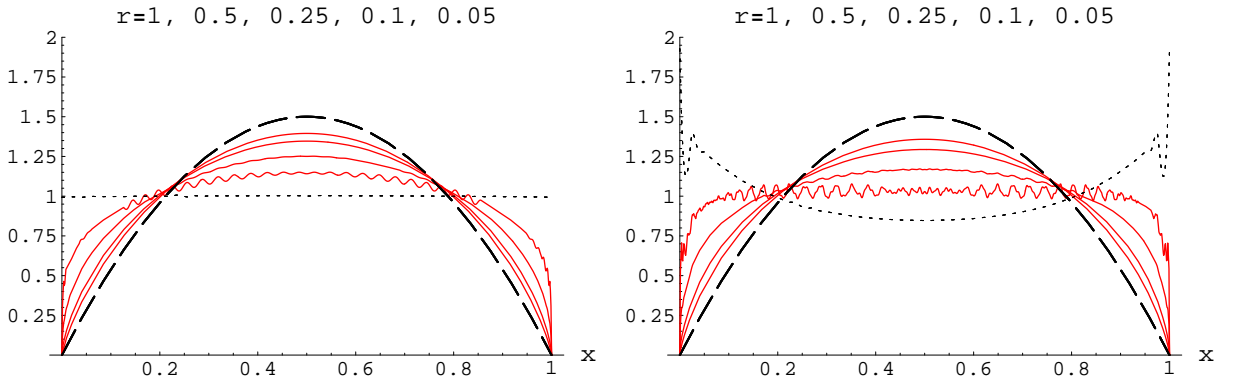


FIG. 9: The LO ERBL evolution of the nonlocal model predictions for the leading-twist *vector* DAs of the photon $\phi_{\parallel\gamma}^{(v)}(x, q^2)$. Left: the real photon DA; right: the virtual photon at $q^2 = 0.25 \text{ GeV}^2$. The dashed lines show the asymptotic DA, $6x(1-x)$. Initial conditions, indicated by dotted lines, are evaluated in the nonlocal quark model at the initial scale $\mu^{\text{inst}} = 530 \text{ MeV}$. The solid lines correspond to evolved DA's at scales $Q = 1, 2.4, 10, \text{ and } 1000 \text{ GeV}$.

which should be compared with the exact result obtained in the local models

$$\psi_\gamma^{(t)\text{SQM}}(x) = \frac{1}{2}(\delta(x) + \delta(1-x)) - \Theta(x\bar{x}). \quad (82)$$

Taking literally these results one gets that the normalization conditions are violated in the WW approximation. Indeed, all $\psi_\gamma^{\text{WW}}(x)$ are normalized to unity. One can fix this problem by shifting the corresponding distributions by constants, forcing the norms for $\psi_\gamma^{(v)\text{WW}}$ and $\psi_\gamma^{(t)\text{WW}}(x)$ to be zero. The corresponding distributions are shown in Figs. 11 and 13.

There were attempts to find photon distribution function within next-to-leading conformal expansion with non-perturbative coefficients determined from the QCD sum rules [39]. To the next-to-leading order in the conformal expansion the twist-3 photon DA were found as

$$\psi_{\gamma\perp}^{(v)}(x) = 5(3\xi^2 - 1) + \frac{3}{64}(15\omega_\gamma^V - 5\omega_\gamma^A)(3 - 30\xi^2 + 35\xi^4), \quad (83)$$

$$\psi_\gamma^{(a)}(x) = \frac{5}{2}(1 - \xi^2)(5\xi^2 - 1)\left(1 + \frac{9}{16}\omega_\gamma^V - \frac{3}{16}\omega_\gamma^A\right), \quad (84)$$

and the twist-4 photon DA

$$h_\gamma(x) = -10(1 + 2\kappa^+)C_2^{1/2}(\xi), \quad (85)$$

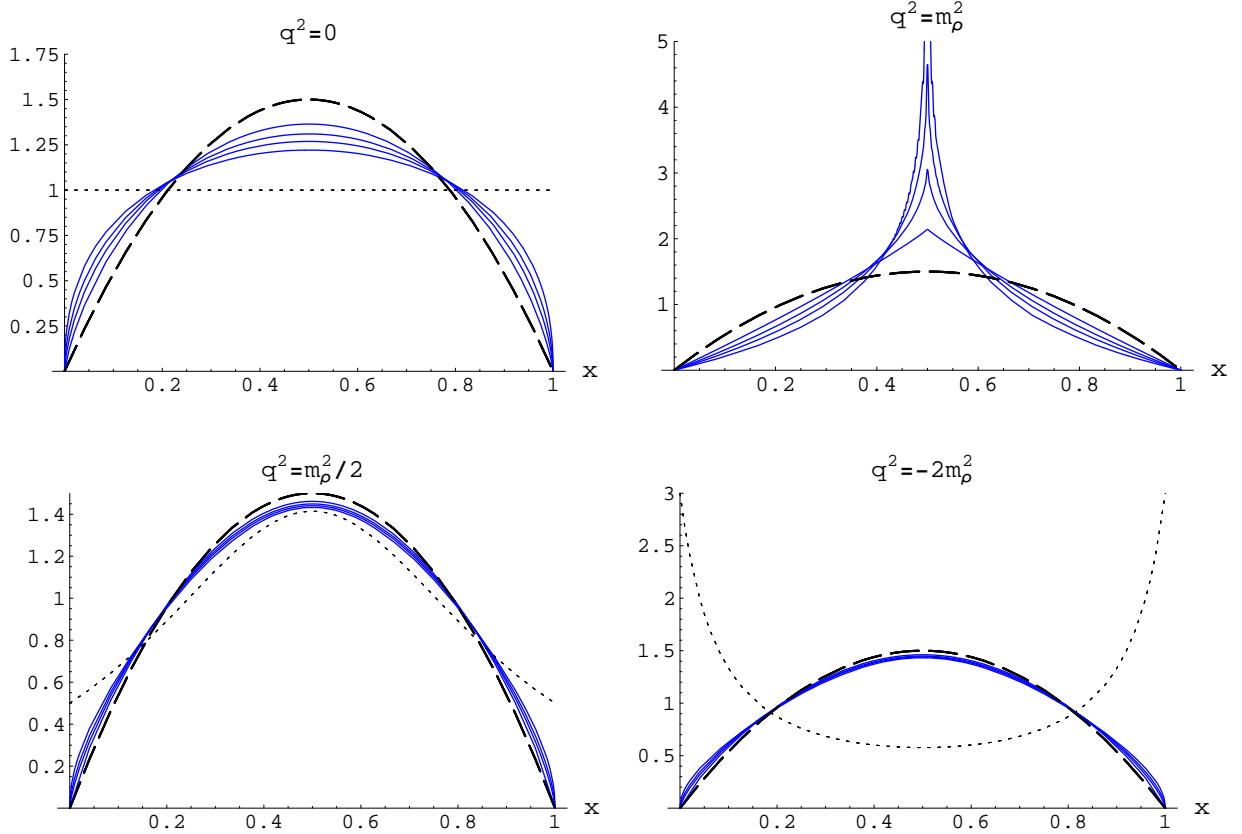


FIG. 10: Evolution of the real photon DA (top left), ρ -meson DA (top right), virtual photon at $q^2 = -m_\rho^2/2$ (bottom left), and virtual photon at $q^2 = 2m_\rho^2$ (bottom right). Initial conditions, indicated by dotted lines, are evaluated in the spectral quark model at the initial scale $\mu^{\text{SQM}} = 313$ MeV. For the ρ -meson case the initial condition is given in Eq. (67). The solid lines correspond to evolved DA's at scales $Q = 1, 2.4, 10, \text{ and } 1000$ GeV. With the larger of the scale the evolved DA is closer to the asymptotic form $6x(1-x)$, plotted with the dashed line. The corresponding values of the evolution ratio r are given in the figures. The appearance of tiny wiggles is a numerical artefact.

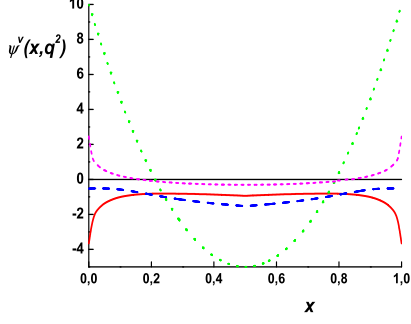


FIG. 11: Dependence of the regular part (without δ -functions) of the twist-3 vector component of the photon DA on transverse momentum squared ($q^2 = 0.25 \text{ GeV}^2$ solid line, $q^2 = 0 \text{ GeV}^2$ dashed line). The short dashed line corresponds to the WW approximation (80) and the dotted line is for the conformal approximation (83)

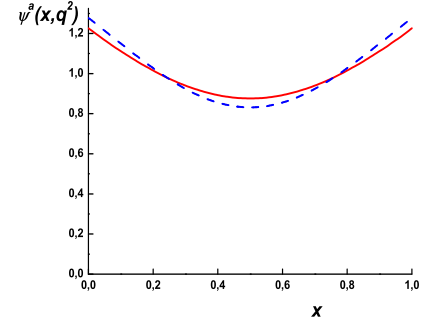


FIG. 12: Dependence of the twist-3 axial component of the photon DA on transverse momentum squared ($q^2 = 0.25 \text{ GeV}^2$ solid line, $q^2 = 0 \text{ GeV}^2$ dashed line)

where the parameters ω_γ^V , ω_γ^A and \varkappa^+ correspond to matrix-elements of local operators of dimension 6. In the vector-dominance approximation they are

$$\omega_\gamma^V = 3.8 \pm 1.8, \quad \omega_\gamma^A = -2.1 \pm 1.0, \quad \varkappa^+ = 0. \quad (86)$$

Note that at low scales the existing QCD sum rule results do not provide reliable results [39].

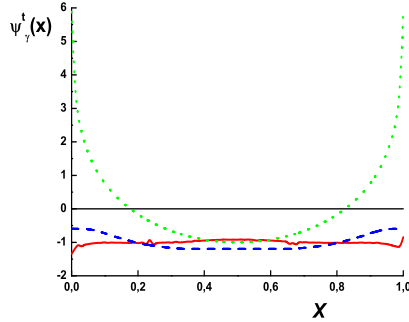


FIG. 13: Dependence of the regular part of the twist-3 tensor component of the photon DA on transverse momentum squared ($q^2 = 0.25 \text{ GeV}^2$ solid line, $q^2 = 0 \text{ GeV}^2$ dashed line, $q^2 = -0.09 \text{ GeV}^2$ short-dashed line). The dotted line is for the WW approximation (81).

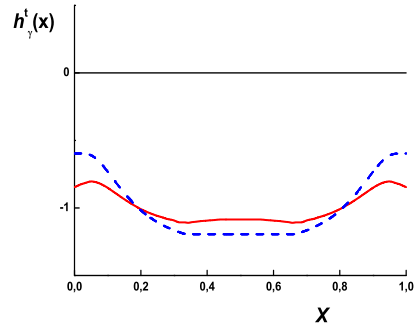


FIG. 14: Dependence of the regular part of the twist-4 tensor component of the photon DA on transverse momentum squared ($q^2 = 0.25 \text{ GeV}^2$ solid line, $q^2 = 0 \text{ GeV}^2$ dashed line)

The QCD evolution of the higher-twist components of the DAs is a very complicated problem. The reason is that unlike the leading-twist case, where the evolution involves the single distribution and leads to simple ERBL equations, the evolution of higher twist components couples the quark bilinears to the three-particle quark-gluon components [9, 38, 66]. At the moment there is no manageable procedure we could promptly use, hence we cannot repeat the evolution calculation for the quark model prediction for non-leading twist DAs. This important problem is interesting in its own right, but it extends outside of the scope of this paper.

VII. CONCLUSIONS

In the present work we have carried out an analysis of the hadronic part of the photon DAs of leading and higher twists up to fourth order at low normalization scale within several effective chiral quark models. We have studied the DAs of real and virtual photons for both transverse and longitudinal polarizations. Our analysis has been performed within two classes of models: the nonlocal model, based on the instanton picture of the QCD vacuum, and local models (the spectral quark model and the Nambu–Jona-Lasinio model). Despite the different nature and details of the calculations, our analysis has shown a remarkable similarity of the results in both classes of models. By working with the photon vertex satisfying the Ward-Takahashi identity we have revised and improved the results for the leading-twist photon DA first performed in [16]. We have shown that the calculations based on the nonlocal model with a correct implementation of gauge invariance resulted in much flatter results, with the photon DA remaining non-zero at the end-points $x = 0, 1$, in qualitative agreement with local quark model calculations.

The main findings may be summarized as follows.

(1) The leading-twist DAs of the real photon at low momenta scale are constant in the local models and almost constant for the nonlocal model. The independence of the photon DAs on x is expected for the local models. They also predict a constant behaviour for the leading-twist pion DA [19]. At the same time the nonlocal model predicts nontrivial x dependence in the case of the pion [13, 17, 36], and shows a constant behaviour for the photon independently on the shape of the nonlocal form factor. This is a consequence of the fact that the photon has no hadronic form factor in contrary to hadrons which are a genuine bound state of dynamical quarks.

(2) Furthermore we show that applying the QCD evolution to leading order of the perturbation theory, the leading-twist photon DAs become immediately zero at the edge points of the x interval (as in the pion case of Ref. [19]) and are always wider (flatter) than the asymptotic DA. At the same time the evolution of the moments of DAs is evidently continuous. This is a typical situation for functional series which are non-uniformly convergent. The role of the QCD evolution is very important, as the quark-model results are far from the asymptotic form. The quark model scale estimated in Ref. [19] for the local models is very low, about 320 MeV, therefore the evolution is very fast. For the instanton model it is estimated as 530 MeV [54, 67]. In short, our predictions may be compared to data only after a suitable QCD evolution has been carried out. Further, for more realistic predictions the perturbative evolution with a kernel calculated at the two-loop level is certainly desirable.

(3) Some of the higher-twist photon DAs have delta-function behaviour at the edge points of the x interval. It might be interpreted as originating from differentiating the constant leading twist DAs and corresponds to the quark-anti-quark configurations of the photon DA when all momentum is carried by one quark (or anti-quark). This singular initial behaviour is washed out during perturbative QCD evolution to higher momentum scales. We also predict the behaviour of the leading- and higher-twist DAs for nonzero virtuality of the photon.

(4) We have drawn our attention to the fact that the equations of motion of perturbative QCD and of the effective approaches are different. In the latter case spontaneous breaking of chiral symmetry is taken into account in terms of a momentum dependent dynamical quark mass. So our results do not coincide with those obtained in perturbative QCD using the equations of motion. In particular, the relations between normalization constants, and DAs for different twist (the Wandzura-Wilczek relations) are not satisfied in the effective approach. We question the validity of such a method, since it implicitly assumes that current quarks are on the mass shell and free, while our interest is in low energy matrix elements. We show that the norm of the tensor amplitude is related to the magnetic susceptibility of the quark condensate, and the zero norm in the vector channel is constrained by the vector-current conservation, while the axial-vector norm remains unconstrained. The latter is determined by nonperturbative dynamics, and therefore its value is model-dependent.

(5) Finally we compare our results with those obtained from the conformal twist expansion [39] using QCD sum rules and vector-meson-dominance methods. It seems that the results obtained in the leading and next-to-leading orders of the conformal expansion do not converge. We have also considered the Wandzura-Wilczek method of estimation of the higher twist DAs assuming a constant distribution in the leading order.

Acknowledgments

AD thanks for partial support from the Russian Foundation for Basic Research projects No. 04-02-16445, Scient. School grant 4476.2006.2 and the JINR Bogoliubov–Infeld program. This research is supported by the Polish Ministry of Education and Science, grants 2P03B 02828 and 2P03B 05925, by the Spanish Ministerio de Asuntos Exteriores and the Polish Ministry of Education and Science, project 4990/R04/05, by the Spanish DGI and FEDER funds with grant no. FIS2005-00810, Junta de Andalucía grant No. FQM-225, and EU RTN Contract CT2002-0311 (EURIDICE).

APPENDIX A: USEFUL INTEGRALS

The calculation in the nonlocal models is most involved, hence we show it first. Formulas for the local models may then be obtained from the nonlocal model expressions as limiting cases, with SQM involving an extra spectral integration. We use the propagator (19) and the vertex (22), and evaluate the Dirac traces in (49) for the tensor component. The electromagnetic vertex is split into the local part and non-local part, according to Eq. (22). We use the identity

$$2k \cdot q = D_+ - D_- + M_+^2 - M_-^2.$$

For the local part we find

$$\int d\tilde{k} \delta(k \cdot n - \frac{1}{2}\xi) \text{Tr}[\sigma_{\alpha\beta} S_+ \gamma \cdot e^{(\lambda)} S_-] = [q_\beta e_\alpha^{(\lambda)} - q_\alpha e_\beta^{(\lambda)}] I_q + [n_\beta e_\alpha^{(\lambda)} - n_\alpha e_\beta^{(\lambda)}] I_n, \quad (\text{A1})$$

with

$$\begin{aligned} I_q &= 4i \int d\tilde{k} \delta(k \cdot n - \frac{1}{2}\xi) \frac{M_+ \bar{x} + M_- x}{D_+ D_-}, \\ I_n &= 2i \int d\tilde{k} \delta(k \cdot n - \frac{1}{2}\xi) \left[(M_+ - M_-) \left(\frac{1}{D_+} - \frac{1}{D_-} \right) \right. \\ &\quad \left. - \frac{(M_+ - M_-)(M_+^2 - M_-^2 + q^2(\bar{x} - x))}{D_+ D_-} \right]. \end{aligned} \quad (\text{A2})$$

The piece involving the nonlocal of the quark-photon interaction vertex has the form

$$\int d\tilde{k} \delta(k \cdot n - \frac{1}{2}\xi) \text{Tr}[\sigma_{\alpha\beta} S(+)\tilde{S}(-)] M_{+,-}^{(1)} (2k - q) \cdot e^{(\lambda)}. \quad (\text{A3})$$

All quantities appearing in the above integrals are functions of squares of momenta, $k^2 = k_+ k_- - u$ and $(k - q)^2 = (k_+ - q_+)(k_- - q_-) - u$, with $u = k_\perp^2$. Since the transverse and $(+-)$ spaces are factorized, for the clarity of notation we introduce $K = (k_0, k_3)$ and $Q = (Q_0, Q_3)$. In order to proceed further it is convenient to pass to the Laplace-transform space

$$\begin{aligned} F_+ &= F(k^2) = \int_0^\infty d\alpha e^{-\alpha K^2} \tilde{F}_\alpha(u), \\ G_- &= G((k - q)^2) = \int_0^\infty d\beta e^{-\beta(K-Q)^2} \tilde{G}_\alpha(u). \end{aligned} \quad (\text{A4})$$

The terms in Eq. (A2) and in other formulas for other observables discussed in this paper have the form of integrals over $\int \delta(k \cdot n - \frac{1}{2}\xi)$ of functions of k^2 , functions of $(k - q)^2$, or the product of the two.

Using the definitions (A4) we find

$$\begin{aligned} \int d^2 K \delta(k \cdot n - \frac{1}{2}\xi) F_+ &= \int d^2 K \int_{-\infty}^\infty \frac{d\lambda}{2\pi} \int_0^\infty d\alpha \tilde{F}_\alpha(u) e^{-\alpha K^2 - i\lambda(k \cdot n - x)} = \\ &= \pi \int \frac{d\lambda}{2\pi} \int \frac{d\alpha}{\alpha} \tilde{F}_\alpha(u) e^{i\lambda x} = \pi \int_0^\infty dz \int d\alpha e^{-\alpha z} \tilde{F}_\alpha(u) \delta(x) = \pi \int dz F_{u+z} \delta(x), \end{aligned} \quad (\text{A5})$$

where on the way we have carried the gaussian integration over $d^2 K$. Similarly,

$$\int d^2 K \delta(k \cdot n - \frac{1}{2}\xi) G_- = \pi \int dz G_{u+z} \delta(\bar{x}).$$

For integrals involving the product of $F_+ G_-$ we have

$$\begin{aligned} \int d^2 K \delta(k \cdot n - \frac{1}{2}\xi) F_+ G_- &= \int d^2 K \int \frac{d\lambda}{2\pi} \int d\alpha \int d\beta \tilde{F}_\alpha(u) \tilde{G}_\beta(u) e^{-\alpha K^2 - \beta(K-Q)^2 - i\lambda(k \cdot n - x)} = \\ &= \pi \int \frac{d\lambda}{2\pi} \int \frac{d\alpha d\beta}{(\alpha + \beta)^2} \tilde{F}_\alpha(u) \tilde{G}_\beta(u) e^{-\frac{\alpha\beta}{\alpha+\beta} q^2 - i\lambda(\frac{\beta}{\alpha+\beta} - x)} = \\ &= \pi \int \frac{d\lambda'}{2\pi} \int \frac{d\alpha d\beta}{(\alpha + \beta)} \tilde{F}_\alpha(u) \tilde{G}_\beta(u) e^{-\frac{\alpha\beta}{\alpha+\beta} q^2 - i\lambda'(\bar{x}\beta - x\alpha)}, \end{aligned} \quad (\text{A6})$$

where $\lambda' = \lambda/(\alpha + \beta)$. Since $\int \frac{d\lambda'}{2\pi} \exp(-i\lambda'(\bar{x}\beta - x\alpha)) = \delta(\bar{x}\beta - x\alpha)$, and $\alpha \geq 0, \beta \geq 0$, we verify that the integral (A6) has the correct support $\sim \Theta(x\bar{x})$.

For the case of real photons, $q^2 = 0$, we have

$$\int d^2 K \delta(k \cdot n - \frac{1}{2}\xi) F_+ G_- \pi \int dz \int \frac{d\lambda}{2\pi} \int d\alpha d\beta \tilde{F}_\alpha(u) \tilde{G}_\beta(u) e^{-(\alpha+\beta)z - i\lambda(\bar{x}\beta - x\alpha)} = \pi \int dz \int \frac{d\lambda}{2\pi} F_{u+z-i\lambda x} G_{u+z+i\lambda \bar{x}}.$$

For the general case of virtual photons one cannot unfold the Laplace transforms. A formula convenient for numerical calculations has the form

$$\int d^2 K \delta(k \cdot n - \frac{1}{2}\xi) F_+ G_- = \pi \int \frac{d\alpha}{\alpha} \tilde{F}_{\bar{x}\alpha}(u) \tilde{G}_{x\alpha}(u) e^{-\alpha x \bar{x} q^2}. \quad (\text{A7})$$

For the case on the non-local vertex we encounter integrands which are no longer separable in the K^2 and $(K-Q)^2$ variables, as they $M^{(1)}$ of Eq. (22). This quantity may be written as

$$M_{+,-}^{(1)} = \int_0^1 dt M'(tK^2 + (1-t)(K-Q)^2 + u),$$

where the prime defines the derivative with respect to the argument. Hence the Laplace transform of $M_{+,-}^{(1)}$ in the variable γ is $-\gamma \tilde{M}(\gamma)$.

We introduce

$$\Delta = \alpha + \beta + \gamma, \quad \alpha' = \alpha + \gamma t, \quad \beta' = \beta + \gamma(1-t).$$

The following integrals are needed in our analysis:

$$\begin{aligned} I_1 &= \int d^2 K \delta(k \cdot n - \frac{1}{2}\xi) F_+ G_- M_{+,-}^{(1)} k \cdot \epsilon^{(\kappa)} = \\ &\int \frac{d\lambda}{2\pi} \frac{d\alpha d\beta d\gamma dt}{\Delta} \tilde{F}_\alpha(u) \tilde{G}_\beta(u) [-\gamma \tilde{M}'_\gamma(u)] e^{-\frac{\alpha'\beta'}{\Delta} q^2 - i\lambda(\beta'\bar{x} - \alpha'x)} \left[-\frac{i}{2} \Delta \lambda n \cdot \epsilon^{(\kappa)} \right] \\ I_2^{\mu\nu} &= \int d^2 K \delta(k \cdot n - x) F_+ G_- M_{+,-}^{(1)} [q^\mu k^\nu - q^\nu k^\mu] k \cdot \epsilon^{(\kappa)} = \\ &\int \frac{d\lambda}{2\pi} \frac{d\alpha d\beta d\gamma dt}{\Delta^2} \tilde{F}_\alpha(u) \tilde{G}_\beta(u) [-\gamma \tilde{M}'_\gamma(u)] e^{-\frac{\alpha'\beta'}{\Delta} q^2 - i\lambda(\beta'\bar{x} - \alpha'x)} \times \\ &\left[\frac{1}{4} (q^\mu \epsilon^{(\kappa),\nu} - q^\nu \epsilon^{(\kappa),\mu}) - \Delta^2 \lambda^2 (q^\mu n^\nu - q^\nu n^\mu) n \cdot \epsilon^{(\kappa)} \right]. \end{aligned} \quad (\text{A8})$$

Carrying the λ integration leads to $\delta(\beta'\bar{x} - \alpha'x)$, which together with the positivity of α' and β' leads to the correct support (A6).

For the case of real photons we find

$$\begin{aligned} I_1 &= 0, \\ I_2^{\mu\nu} &= \int dz z \int \frac{d\lambda}{2\pi} F_{u+z-i\lambda x} G_{u+z+i\lambda \bar{x}} M_{u+z-i\lambda x, u+z+i\lambda \bar{x}}^{(1)} \frac{1}{4} (q^\mu \epsilon^{(\kappa),\nu} - q^\nu \epsilon^{(\kappa),\mu}). \end{aligned} \quad (\text{A9})$$

APPENDIX B: GAUSSIAN NONLOCALITY

In this appendix we collect some useful relations valid for Gaussian shape of the nonlocal function $f(p)$ which provides the expression for the dynamical mass as (in chiral limit)

$$M(p^2) = M_0 \exp(-2p^2/\Lambda^2). \quad (\text{B1})$$

It is important to stress that exponentially decreasing function at large Euclidean momenta is a direct consequence of requirements of the gauge invariance and continuity of nonlocal matrix elements [15, 54]. First of all consider the propagator function

$$P(p^2) = \frac{1}{p^2 + M_0^2 \exp(-4p^2/\Lambda^2)} = \frac{1}{M_0^2} \frac{1}{\tilde{p}^2 + \exp(-4\tilde{p}^2 y^2)}, \quad (\text{B2})$$

where the second equation is rewritten in the dimensionless variable $\tilde{p} = p/M_0$, with $y = M_0/\Lambda$. Depending on the values of parameters M_0 and Λ the function P may or may not have a real pole. The critical value is obtained from equating denominator and its derivative in p^2 to zero. Then one gets the region of parameters where the propagator has no poles at real values of p^2 as [32, 68]

$$y > y_0 = 1/(2\sqrt{e}) \approx 0.303. \quad (\text{B3})$$

In the other region, $y < y_0$, the real valued pole appears at

$$p_0^2 = -4\kappa M_0^2, \quad (\text{B4})$$

where the coefficient κ monotonically changes between $\kappa = 1$ obtained in the local limit $y \rightarrow 0$ and $\kappa = \sqrt{e}$ reached at the critical point $y \rightarrow y_0$.

In the present paper in the nonlocal model we use the parameters (27) corresponding to $y^* = 0.195$, where the pole (B4) appears with $\kappa = 1.13$ at $p_0^2 = -0.29 \text{ GeV}^2$. This is a reason why our calculations are given in the region far away from the pole. The chosen value of the vector coupling G_V corresponds to the ρ -meson mass at the somewhat low pole position of $M_\rho = 541 \text{ MeV}$.

The propagator function has also an infinite number of complex valued poles (a similar situation is also encountered in the NJL model with the proper-time regularization [69]). This fact makes it difficult to carry out calculations of integrals directly in the momentum space. A big advantage is to transform all integrals to the α -representation where some analytical calculation may be done [15, 70]. To this end we expand (B2) as

$$P(s) = \frac{1}{s} \sum_{k=-0}^{\infty} \left(\frac{-M_0^2 \exp(-4s/\Lambda^2)}{s} \right)^k \quad (\text{B5})$$

and apply the Laplace transforms

$$\frac{1}{s} \Rightarrow 1, \quad \frac{1}{s^k} e^{-As} \Rightarrow \frac{(\alpha - A)^{k-1}}{(k-1)!} \Theta(\alpha - A)$$

to each term of the expansion. Then one gets the α -representation of the propagator function

$$P(s) \Rightarrow \tilde{P}(\alpha) = 1 + \sum_{k=1}^{\infty} \frac{[-M_0^2 (\alpha - 4k/\Lambda^2)]^k}{k!} \Theta(\alpha - 4k/\Lambda^2). \quad (\text{B6})$$

This transformation may be done for all functions. For example, one has transformation

$$P_f(s) = \frac{\exp(-s/\Lambda^2)}{s + M_0^2 \exp(-4s/\Lambda^2)} \Rightarrow \tilde{P}_f(\alpha) = \sum_{k=1}^{\infty} \frac{[-M_0^2 (\alpha - (4k-3)/\Lambda^2)]^{k-1}}{(k-1)!} \Theta(\alpha - (4k-3)/\Lambda^2). \quad (\text{B7})$$

The functions $\tilde{P}(\alpha)$ and $\tilde{P}_f(\alpha)$ are presented in Fig. 15. Let us note some general properties of the transformed functions. At small α one has $\tilde{P}(0) = 1$ because large s asymptotic $P(s \rightarrow \infty) = 1/s$. In fact for Gaussian function $f(p^2)$ from (B6) and (B7) one has $\tilde{P} = 1$ in the interval $\alpha \in [0, 4/\Lambda^2]$. At the same time $\tilde{P}_f(0) = 0$, since at large s the function $P_f(s)$ decreases faster than $1/s$. More precisely one has for Gaussian function $\tilde{P}_f(\alpha) = 0$ at $\alpha \in [0, 1/\Lambda^2]$ and $\tilde{P}_f(\alpha) = 1$ at $\alpha \in [1/\Lambda^2, 5/\Lambda^2]$.

The asymptotic behavior at large α depends on the position of the pole closest to the real axis of the function in the s space. In the region of parameters (B3) it is defined by the complex pole and has an oscillating character modulated by the exponential decay. The similar relation between "confining" (better to say screening) properties of propagator and complex singularities of the propagators in momentum space has been obtained in [71] for QED in three-dimensions for the fermion propagator and in [53] for QCD in the instanton model for the gluon field strength correlator.

For the set of parameters $y < y_0$ the large α asymptotic of $\tilde{P}(\alpha)$ is purely exponential

$$\tilde{P}(\alpha) \sim \exp(-\kappa M_0^2 \alpha). \quad (\text{B8})$$

The function $\tilde{P}_f(\alpha)$ has the same asymptotics because in the s space it has the same dominating singularity. Through the use of the α -representation we avoid complexities typical for the momentum integral calculations.

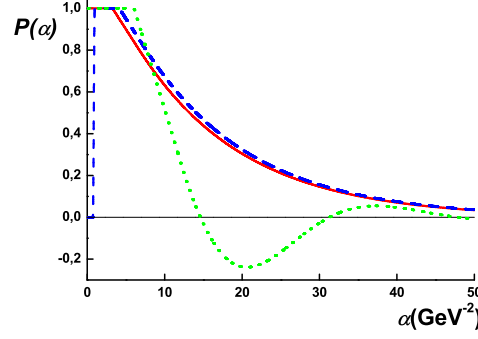


FIG. 15: The propagator functions P (solid line) and P_f (dashed line) in α -representation. The α -representation of the propagator function P for "confining" set of parameters ($M_0 = 350$ MeV, $\Lambda = 815$ MeV) is given by dotted line.

APPENDIX C: QCD EVOLUTION

Here we collect the formulas needed for the leading-order QCD evolution. The Gegenbauer coefficients evolve as

$$a_n^i(Q^2) = a_n^i(Q_0^2) \left(\frac{\alpha(Q^2)}{\alpha(Q_0^2)} \right)^{(\gamma_n^i - \gamma_0^i)/(2\beta_0)} \quad (\text{C1})$$

$$a_n^i(Q_0^2) = c_n^m \int_0^1 dx C_n^m(2x-1) \phi^i(x, Q_0^2), \quad (\text{C2})$$

with

$$\begin{aligned} c_n^{3/2} &= \frac{2}{3} \frac{2n+3}{(n+1)(n+2)} \\ c_n^{1/2} &= 2n+1. \end{aligned} \quad (\text{C3})$$

The anomalous dimensions are as follows (see for example in [72]):

$$\begin{aligned} \gamma_n^T &= -\frac{8}{3} \left[3 - 4 \sum_{k=1}^{n+1} \frac{1}{k} \right], \\ \gamma_n^V &= \gamma_n^{\text{AV}} = -\frac{8}{3} \left[3 + \frac{2}{(n+1)(n+2)} - 4 \sum_{k=1}^{n+1} \frac{1}{k} \right], \\ \gamma_n^{\text{PS}} &= -\frac{8}{3} \left[3 + \frac{8}{(n+1)(n+2)} - 4 \sum_{k=1}^{n+1} \frac{1}{k} \right]. \end{aligned} \quad (\text{C4})$$

-
- [1] A. V. Belitsky and A. V. Radyushkin, Phys. Rept. **418**, 1 (2005), hep-ph/0504030.
 - [2] A. V. Radyushkin, JINR report JINR-P2-10717, arXiv:hep-ph/0410276 (1977).
 - [3] A. V. Efremov and A. V. Radyushkin, Theor. Math. Phys. **42**, 97 (1980).
 - [4] A. V. Efremov and A. V. Radyushkin, Phys. Lett. **B94**, 245 (1980).
 - [5] G. P. Lepage and S. J. Brodsky, Phys. Lett. **B87**, 359 (1979).
 - [6] G. P. Lepage and S. J. Brodsky, Phys. Rev. **D22**, 2157 (1980).
 - [7] V. L. Chernyak and A. R. Zhitnitsky, Nucl. Phys. **B201**, 492 (1982).
 - [8] S. V. Mikhailov and A. V. Radyushkin, JETP Lett. **43**, 712 (1986).
 - [9] V. M. Braun and I. E. Filyanov, Z. Phys. **C44**, 157 (1989).
 - [10] A. P. Bakulev and S. V. Mikhailov, Z. Phys. **C68**, 451 (1995), hep-ph/9412366.
 - [11] S. S. Agaev, Phys. Rev. **D69**, 094010 (2004), hep-ph/0403161.

- [12] A. S. Bagdasaryan, S. V. Esaibegian, and N. L. Ter-Isaakian, *Yad. Fiz.* **42**, 440 (1985).
- [13] S. V. Esaibegian and S. N. Tamarian, *Sov. J. Nucl. Phys.* **51**, 310 (1990).
- [14] A. E. Dorokhov, *Nuovo Cim.* **A109**, 391 (1996).
- [15] A. E. Dorokhov and L. Tomio, *Phys. Rev.* **D62**, 014016 (2000).
- [16] V. Y. Petrov, M. V. Polyakov, R. Ruskov, C. Weiss, and K. Goeke, *Phys. Rev.* **D59**, 114018 (1999), hep-ph/9807229.
- [17] A. E. Dorokhov, *JETP Lett.* **77**, 63 (2003), hep-ph/0212156.
- [18] M. Praszalowicz and A. Rostworowski, *Phys. Rev.* **D64**, 074003 (2001), hep-ph/0105188.
- [19] E. Ruiz Arriola and W. Broniowski, *Phys. Rev.* **D66**, 094016 (2002), hep-ph/0207266.
- [20] S. Dalley and B. van de Sande, *Phys. Rev.* **D67**, 114507 (2003), hep-ph/0212086.
- [21] L. Del Debbio, M. Di Pierro, and A. Dougall, *Nucl. Phys. Proc. Suppl.* **119**, 416 (2003), hep-lat/0211037.
- [22] L. Del Debbio, *Few Body Syst.* **36**, 77 (2005).
- [23] M. Gockeler *et al.*, (2005), hep-lat/0510089.
- [24] D. Ashery, *Prog. Part. Nucl. Phys.* **56**, 279 (2006).
- [25] N. N. Nikolaev, W. Schafer, and G. Schwiete, *Phys. Rev.* **D63**, 014020 (2001), hep-ph/0009038.
- [26] V. M. Braun, D. Y. Ivanov, A. Schafer, and L. Szymanowski, *Phys. Lett.* **B509**, 43 (2001), hep-ph/0103275.
- [27] S. J. Brodsky, L. Frankfurt, J. F. Gunion, A. H. Mueller, and M. Strikman, *Phys. Rev.* **D50**, 3134 (1994), hep-ph/9402283.
- [28] V. M. Braun, S. Gottwald, D. Y. Ivanov, A. Schafer, and L. Szymanowski, *Phys. Rev. Lett.* **89**, 172001 (2002), hep-ph/0206305.
- [29] E791, E. M. Aitala *et al.*, *Phys. Rev. Lett.* **86**, 4773 (2001), hep-ex/0010044.
- [30] ZEUS, J. M. Ukleja, *Eur. Phys. J.* **C33**, s506 (2004).
- [31] H1, N. Coppola, (2004), hep-ex/0410057.
- [32] R. D. Bowler and M. C. Birse, *Nucl. Phys.* **A582**, 655 (1995), hep-ph/9407336.
- [33] I. V. Anikin, A. E. Dorokhov, and L. Tomio, *Phys. Part. Nucl.* **31**, 509 (2000).
- [34] A. E. Dorokhov and W. Broniowski, *Eur. Phys. J.* **C32**, 79 (2003), hep-ph/0305037.
- [35] E. Ruiz Arriola and W. Broniowski, *Phys. Rev.* **D67**, 074021 (2003), hep-ph/0301202.
- [36] I. V. Anikin, A. E. Dorokhov, and L. Tomio, *Phys. Lett.* **B475**, 361 (2000), hep-ph/9909368.
- [37] E. R. Arriola and W. Broniowski, (2006), hep-ph/0605318.
- [38] P. Ball, V. M. Braun, Y. Koike, and K. Tanaka, *Nucl. Phys.* **B529**, 323 (1998), hep-ph/9802299.
- [39] P. Ball, V. M. Braun, and N. Kivel, *Nucl. Phys.* **B649**, 263 (2003), hep-ph/0207307.
- [40] A. Ali and V. M. Braun, *Phys. Lett.* **B359**, 223 (1995), hep-ph/9506248.
- [41] P. Ball and V. M. Braun, *Phys. Rev.* **D54**, 2182 (1996), hep-ph/9602323.
- [42] J. Terning, *Phys. Rev.* **D44**, 887 (1991).
- [43] B. Holdom, *Phys. Rev.* **D45**, 2534 (1992).
- [44] R. S. Plant and M. C. Birse, *Nucl. Phys.* **A628**, 607 (1998), hep-ph/9705372.
- [45] W. Broniowski, (1999), hep-ph/9909438.
- [46] E. V. Shuryak, *Nucl. Phys.* **B203**, 93 (1982).
- [47] D. Diakonov and V. Y. Petrov, *Nucl. Phys.* **B245**, 259 (1984).
- [48] N. I. Kochelev, *Yad. Fiz.* **41**, 456 (1985).
- [49] A. E. Dorokhov, Y. A. Zubov, and N. I. Kochelev, *Sov. J. Part. Nucl.* **23**, 522 (1992).
- [50] C. D. Roberts and A. G. Williams, *Prog. Part. Nucl. Phys.* **33**, 477 (1994), hep-ph/9403224.
- [51] S. V. Mikhailov and A. V. Radyushkin, *Phys. Rev.* **D45**, 1754 (1992).
- [52] A. E. Dorokhov, S. V. Esaibegian, and S. V. Mikhailov, *Phys. Rev.* **D56**, 4062 (1997), hep-ph/9702417.
- [53] A. E. Dorokhov, S. V. Esaibegian, A. E. Maximov, and S. V. Mikhailov, *Eur. Phys. J.* **C13**, 331 (2000), hep-ph/9903450.
- [54] A. E. Dorokhov, *Eur. Phys. J.* **C42**, 309 (2005), hep-ph/0505007.
- [55] A. E. Dorokhov and L. Tomio, (1998), hep-ph/9803329.
- [56] A. E. Dorokhov, *Phys. Rev.* **D70**, 094011 (2004), hep-ph/0405153.
- [57] J. Gasser and H. Leutwyler, *Ann. Phys.* **158**, 142 (1984).
- [58] H.-C. Kim, M. Musakhanov, and M. Siddikov, *Phys. Lett.* **B608**, 95 (2005), hep-ph/0411181.
- [59] A. L. Kataev, G. Parente, and A. V. Sidorov, *Phys. Part. Nucl.* **34**, 20 (2003), hep-ph/0106221.
- [60] A. P. Bakulev, S. V. Mikhailov, and N. G. Stefanis, *Phys. Rev.* **D67**, 074012 (2003), hep-ph/0212250.
- [61] E. Megias, E. Ruiz Arriola, L. L. Salcedo, and W. Broniowski, *Phys. Rev.* **D70**, 034031 (2004), hep-ph/0403139.
- [62] G. V. Efimov and M. A. Ivanov, Bristol, UK: IOP (1993) 177 p.
- [63] O. V. Teryaev, *Phys. Part. Nucl.* **35**, S24 (2004).
- [64] R. M. Davidson and E. Ruiz Arriola, *Phys. Lett.* **B348**, 163 (1995).
- [65] D. Mueller, *Phys. Rev.* **D51**, 3855 (1995), hep-ph/9411338.
- [66] A. S. Gorsky, *Sov. J. Nucl. Phys.* **41**, 275 (1985).
- [67] A. E. Dorokhov, *JETP Lett.* **82**, 1 (2005), hep-ph/0505196.
- [68] G. Ripka, Oxford, UK: Clarendon Pr. (1997) 205 p.
- [69] W. Broniowski, G. Ripka, E. Nikolov, and K. Goeke, *Z. Phys.* **A354**, 421 (1996), hep-ph/9509363.
- [70] I. V. Anikin, A. E. Dorokhov, A. E. Maksimov, L. Tomio, and V. Vento, *Nucl. Phys.* **A678**, 175 (2000).
- [71] P. Maris, *Phys. Rev.* **D52**, 6087 (1995), hep-ph/9508323.
- [72] M. A. Shifman and M. I. Vysotsky, *Nucl. Phys.* **B186**, 475 (1981).